Journal of Solid Mechanics Vol. 7, No. 1 (2015) pp. 96-120

Nonlinear Instability of Coupled CNTs Conveying Viscous Fluid

A. Ghorbanpour Arani [1, 2,*], S. Amir [1]

[1] *Faculty of Mechanical Engineering, University of Kashan, Kashan , Islamic Republic of Iran*
[2] *Institute of Nanoscience & Nanotechnology, University of Kashan, Kashan, Islamic Republic of Iran*

Received 28 October 2014; accepted 29 December 2014

ABSTRACT
In the present study, nonlinear vibration of coupled carbon nanotubes (CNTs) in presence of surface effect is investigated based on nonlocal Euler-Bernoulli beam (EBB) theory. CNTs are embedded in a visco-elastic medium and placed in the uniform longitudinal magnetic field. Using von Kármán geometric nonlinearity and Hamilton's principle, the nonlinear higher order governing equations are derived. The differential quadrature (DQ) method is applied to obtain the nonlocal frequency of coupled visco-CNTs system. The effects of various parameters such as the longitudinal magnetic field, visco-Pasternak foundation, Knudsen number, surface effect, aspect ratio and velocity of conveying viscous are specified. It is shown that the longitudinal magnetic field is responsible for an up shift in the frequency and an improvement of the instability of coupled system. Results also reveal that the surface effect and internal conveying fluid plays an important role in the instability of nano coupled system. Also, it is found that trend of figures have good agreement with previous researches. It is hoped that the nonlinear results of this work could be used in design and manufacturing of nano/micro mechanical system in advanced nanomechanics applications where in this study the magnetic field is a controller parameter.

Keywords: Nonlinear vibration; Coupled system; Magnetic field; Conveying fluid; Surface stress; Knudsen number

1 INTRODUCTION

CNTs are as one of the stable families of nanostructures where they are becoming the most promising material for nano-electronics, nano-devices and nano-composites because of their enormous application such as nano-pipettes, actuators, reactors, fluid filtration devices, targeted drug delivery devices and scanning ion conductance microscopy [1-2]. Due to its potential, nanotubes are used in nano technology, particularly in recent years utilized in vibration of CNTs with/without conveying fluid.

In this regard, Zhen and Fang [3] investigated the nonlocal thermal vibration single-walled carbon nanotubes (SWCNTs) conveying fluid where an elastic beam model developed for analysis of dynamical behavior of fluid conveying SWCNTs. Their results showed that the natural frequencies and critical flow velocity increase as the temperature changes increase. The nonlocal-model's natural frequencies were smaller than the local model's natural frequencies at all temperature changes and flow velocities considered. Vibration analysis of double-walled carbon

* Corresponding author. Tel.: +98 31 55912450; Fax: +98 31 55912424.
E-mail address: aghorban@kashanu.ac.ir (A. Ghorbanpour Arani).

nanotubes (DWCNTs) based on nonlinear EBB and nonlocal elasticity theories was studied by Fang et al. [4]. They considered clamped-clamped condition and used Hamilton's principle to drive nonlinear equations of motion. The influences of nonlocal parameters, nonlinear Van-der-Waals forces, aspect ratio and Winkler constant were discussed on nonlinear coaxial and non co axial vibration. Wang and Ni [5] used EB classical beam to modeling the nanotubes as a continuum structure conveying viscous fluid. They found that the effect of fluid viscosity on the vibration and instability of CNTs can be ignored but increasing the velocity of flow fluid has remarkable effect on the frequency and stability of CNTs. A nonlinear model developed for the flow-induced frequency of a SWCNT by Soltani and Farshidianfar [6], who solved the nonlinear equation of motion by the energy balance method. They indicated that the nonlinearity of the model can be effectively tuned by applying axial tension to the nanotube. Ghorbanpour Arani et al. [7] developed nonlinear vibration and stability of a smart composite micro-tube made of Poly-vinylidene fluoride reinforced by Boron-Nitride nanotubes (BNNTs) embedded in an elastic medium under electro-thermal loadings. The microtube conveyed a fully developed isentropic, incompressible and irrotational fluid flow. Their results indicated that increasing mean flow velocity considerably increases the nonlinearity effects so that small scale and temperature change effects become negligible. It had also been found that stability of the system was strongly dependent on the imposed electric potential and the volume percent of BNNTs reinforcement.

Knudsen number (K_n) is the dimensionless ratio that introduced mean free path of the fluid molecules to a characteristic length of the flow geometry and it is used as a discriminate for identifying the different flow regimes [8]. The effects of Knudsen-dependent nano flow velocity on vibrations of EBB nano-pipe conveying fluid investigated by Mirdamadi et al. [8] and Rashidi et al. [9] who reformulated Navier–Stokes equations, with modified versions of Kn-dependent flow velocity. They found that the Knudsen number has dominated influence on the critical flow velocity and stability of nano structure conveying fluid.

Recently, it has become clear that when materials and structures shrink to nanometers, surface effects often play a critical role in their static or dynamical behavior due to increasing ratio of surface/inter face area to volume. Wang [10] presented an analytical model for predicting inner and outer layers effects on the free vibration of fluid-conveying nanotubes based on the non-local elasticity theory. They indicated that the surface effects with positive elastic constant or positive residual surface tension tend to increase the natural frequency and critical flow velocity. Based on type of continuum elasticity theory, the surface stresses are simulated as a mathematical thin layer that thickness can be neglected with different material properties from the underlying bulk which is completely bonded by the membrane. They proposed the following general and simple expression for surface stress–strain relation. [11, 12]. In spite of many researches about behavior of CNTs using nonlocal elasticity theory, there are limited studies that consider nonlocal visco-elastic systems. Lei et al. [13] presented the dynamic behavior of nonlocal visco-elastic damped nanobeams where the Kelvin–Voigt visco-elastic model was employed to establish the governing equations for the bending vibration of nanotubes. They used transfer function method to obtain the natural frequencies and response functions. The flexural vibration of visco-elastic CNTs conveying fluid and embedded in viscous fluid based on Timoshenko beam (TB) elasticity theory investigated by Ghavanloo and Fazelzadeh [14] who demonstrated increasing visco-elastic structural damping coefficient decreases the critical flow velocity.

It has been proved that the CNTs deform when subjected to the magnetic field due to changes in their magnetic state. There are some studies dealing with on the magneto-elastic behavior of such components in the literatures. Murmu et al. [15] reported an analytical approach to study the effect of a longitudinal magnetic field on the transverse vibration of a magnetically sensitive DWCNT based on nonlocal elasticity theory. Results revealed that presence of a longitudinal magnetic field increases the natural frequencies of the DWCNT. They studied the influence of small scale effects, temperature change, Winkler constant and vibration modes of CNT on the natural frequency. Wang et al. [16] studied the effects of magnetic field and elastic medium on wave propagation in CNTs. They showed that the longitudinal magnetic field increases the velocity wave propagation in some frequency regions where the longitudinal magnetic field has obvious influence on the velocity of wave propagation in CNTs. The behavior of nanoplates under an external in-plane magnetic field based on nonlocal elasticity theory is investigated by Murmu et al. [17], who found that the in-plane magnetic field increases the natural frequencies of the single layer grapheme sheet.

Murmu and Adhikari [18] investigated nonlocal vibration analysis of double nano beam systems and obtained governing equations of motion for EBB model in terms of displacements. They solved the coupled equations by the new analytical method to decouple the set of partial differential equations and they showed that small scale parameters and stiffness of the coupling springs have important role in stability of double nanobeams system. Also these researchers [19, 20] investigated the effects of small scale parameter on the transverse and longitudinal vibration of double nanobeams system. Later Murmu and Adhikari [21] reported nonlocal vibration of double nanoplate system where two single layered grapheme sheets coupled by polymer matrix. They used explicit closed-form expressions for natural frequencies for the case when all four ends are simply-supported. They showed the effect of stiffness elastic medium, small scale parameter, aspect ratio and higher modes on the natural frequencies of coupled system based on an analytical method. Recently, GhorbanpourArani and Amir [22] investigated electro-thermal vibration of double BNNTs which are coupled by elastic medium using strain gradient theory. Two BNNTs are placed in the uniform temperature and electric fields, the latter being applied through attached electrodes at both ends. Moreover, one of the BNNTs oscillates under flow fluid. They derived the higher-order equations of motion base on the Hamilton's principle to obtain the frequency of coupled BNNTs system.

In this study, nonlinear vibration and stability of a double visco-CNTs system based on EBB theory under longitudinal magnetic field with surface effect, conveying fluid is considered. Using Hamilton's principle, the couple governing equations are derived and DQM is presented to estimate the frequency and critical fluid velocity of double bonded visco-CNTs. Several effects of fluid flow on the vibration behavior of the coupled system are investigated thoroughly; moreover the effects of other parameters such as small scale, surface effect, magnetic field and visco-elastic medium modulus are discussed in details.

2 GOVERNING EQUATIONS OF COUPLED SYSTEM

According to the Eringen's nonlocal elasticity model [23, 24], the stress state at a reference point in the body is regarded to be dependent not only on the strain state at this point but also on the strain states at all of the points throughout the body. On the other contract, at the local elasticity theory, the stress state at any point corresponds to the strain state at this point. The constitutive equations of the partial nonlocal elasticity can be considered as:

$$\left(1-(e_0a)\nabla^2\right)\sigma^{\text{Nonlocal}}=\tau^{\text{Local}}, \tag{1}$$

where the right hand of Eq. (1) denotes the classical stress and e_0a is *a* constant parameter showing the small scale effect. In the present model, the nonlocal stress $\left(\sigma^{Nonlocal}\right)$, the corresponding strain ε_{xx}. Using above assumptions for the EBB model, Eq. (1) can be obtained as:

$$\left[1-(e_0a)^2\nabla^2\right]\sigma_{xx}^{\text{Nonlocal}}=E\,\varepsilon_{xx}=\tau_{xx}^{\text{Local}}. \tag{2}$$

The geometry of the system and its surrounding medium are demonstrated in Fig. 1. This figure shows a double visco elastic CNT system which coupled by visco-Pasternak foundations with length l, radius r and effective tubes thickness h that CNTs are contain of fluid flow. In this study CNTs are simulated by EBB model where this simulation can be suitable for CNTs, therefore the displacement filed based on the EBB theory becomes [6]:

$$\begin{aligned}
&\tilde{U}(x,z,t)=U(x,t)-z\frac{\partial W(x,t)}{\partial x},\\
&\tilde{V}(x,z,t)=0,\\
&\tilde{W}(x,z,t)=W(x,t).
\end{aligned} \tag{3}$$

Using Eq. (3), where $\tilde{U}(x,t),\tilde{W}(x,t)$ and $\tilde{V}(x,t)$ are displacement components of middle surface and nonlinear strain displacement relation can be written:

$$\varepsilon_{xx}=\frac{\partial U}{\partial x}-z\frac{\partial^2 W}{\partial x^2}+\frac{1}{2}\left(\frac{\partial W(x,t)}{\partial x}\right)^2. \tag{4}$$

According to Kelvin–Voigt visco elastic model [13] at real life, nano structure mechanical properties depend on the time variation. Therefore, based on this model and nonlocal elasticity model, the nonlocal visco-elastic constitutive relation for EBB can be written as [13]:

$$\sigma_{xx}^{\mathrm{Nonlocal}} - (e_0 a)^2 \frac{\partial^2 \sigma_{xx}^{\mathrm{Nonlocal}}}{\partial x^2} = E\left(1 + g\frac{\partial}{\partial t}\right)\varepsilon_{xx}, \tag{5}$$

where *E* and *g* are Young's modulus and damping coefficient, respectively. In this study, the energy method is used to derive higher order governing equations of motion where total potential energy, $\prod$ is expressed as [25]:

$$\prod = U_s - (K + \Omega), \tag{6}$$

where U_s is strain energy, *K* is total kinetic energy and Ω is the total external work in coupled system. Therefore, the motion equations of embedded visco-elastic coupled CNTs conveying viscose fluid can be derived by Hamilton's principle given as follows [25]:

$$\int_{t_0}^{t_1} \left[\delta U_s - \left(\delta K_{nanotubes} + \delta K_{fluid} + \delta\Omega_{visco-Pasternak} + \delta\Omega_{fluid} + \delta\Omega_{Lorentz}\right)\right] dt = 0, \tag{7}$$

where strain energy of nanotubes are [25]:

$$U_s = \frac{1}{2}\int_0^L \int_{A_i} (\sigma_{xxi}\varepsilon_{xxi})\, dA_i dx, \tag{8}$$

Subscript *i* denotes the number of nanotube where i=1,2 demonstrate upper and lower nanotubes, respectively. Substituting Eq. (4) in Eq. (8), total strain energy is defined as:

$$U_s = \frac{1}{2}\int_0^L \left[\int_{A_i} \sigma_{xxi}\left\{\frac{\partial U_i}{\partial x} + \frac{1}{2}\left(\frac{\partial W_i(x,t)}{\partial x}\right)^2 - z\frac{\partial^2 W_i}{\partial x^2}\right\} dA_i\right] dx, \tag{9}$$

and introducing forces and moments at the intermediate of CNTs as follow:

$$\begin{cases} N_{xi}^{Local} = \int_{A_i} \tau_{xxi}^{Local} dA_i \quad , \quad M_{xi}^{Local} = \int_{A_i} \tau_{xxi}^{Local} z\, dA_i, \\ N_{xi}^{Nonlocal} = \int_{A_i} \sigma_{xxi}^{Nonlocal} dA_i \ , \ M_{xi}^{Nonlocal} = \int_{A_i} \sigma_{xxi}^{Nonlocal} z dA_i \end{cases}. \tag{10}$$

Total strain energy of nanotubes is rewritten as:

$$U_s = \frac{1}{2}\int_0^L \left\{-M_{(xi)}^{NL} \frac{\partial^2 W_i}{\partial x^2} + \frac{1}{2} N_{(xi)}^{NL}\left(\frac{\partial W_i}{\partial x}\right)^2 + N_{(xi)}^{NL} \frac{\partial U_i}{\partial x}\right\} dx, \tag{11}$$

and the total kinetic energy nanotubes can be expressed as [26, 27]:

$$K_{nanotubes} = \frac{1}{2}\rho_t \int_0^L \left\{\int_{A_i} \left[\left(\frac{\partial \tilde{U}_i}{\partial t}\right)^2 + \left(\frac{\partial \tilde{W}_i}{\partial t}\right)^2\right] dA_i\right\} dx. \tag{12}$$

This velocity vector for the transmission fluid through the tubes in beam model can be expressed as [27, 26]:

$$V_x = \frac{\partial \tilde{U}_1}{\partial t} + U_f \cos\theta \quad , \quad V_z = \frac{\partial \tilde{W}_1}{\partial t} - U_f \sin\theta. \tag{13}$$

Work done of the fluid caused by the curvature of the CNT:

$$\delta\Omega_{fluid} = -\int_0^L \int_{A_f} \left\{ \rho_f V_f^2 \frac{\partial^2 W_i}{\partial x^2} \cos\theta \; \delta W_i + \rho_f V_f^2 \frac{\partial^2 W_i}{\partial x^2} \sin\theta \; \delta U_i \right\} dA_f \, dx, \tag{14}$$

where $\theta = -\partial W / \partial x$ and U_f is the constant velocity of fluid and kinetic energy of flow fluid is:

$$K_{fluid} = \frac{1}{2} \rho_f \int_0^L \int_{A_f} \left\{ \left(\frac{\partial \tilde{U}_1}{\partial t} + U_f \cos\theta \right)^2 + \left(\frac{\partial \tilde{W}_1}{\partial t} - U_f \sin\theta \right)^2 \right\} dA_f dx. \tag{15}$$

According to the fluid viscosity effect of CNT, the Navier–stokes equation given as follows [28]:

$$\rho_f \frac{d\vec{V}}{dt} = -\nabla \vec{P} + \mu \nabla^2 \vec{V}. \tag{16}$$

Substituting the fluid velocity vector in Eqs. (15-14), Navier-stokes equations in x, z directions given as follows:

$$\rho_f \left[\frac{\partial}{\partial t} + V_f \frac{\partial}{\partial x} \right] \left[\frac{\partial \tilde{U}}{\partial t} + V_f \cos\theta \right] = -\frac{\partial P}{\partial x} + \mu \frac{\partial^2}{\partial x^2} \left[\frac{\partial \tilde{U}}{\partial t} + V_f \cos\theta \right], \xrightarrow{\int_{A_f} \rho_f dA_f} \tag{17a}$$

$$\rho_f \left[\frac{\partial}{\partial t} + V_f \frac{\partial}{\partial x} \right] \left[\frac{\partial W}{\partial t} - V_f \sin\theta \right] = -\frac{\partial P}{\partial z} + \mu \frac{\partial^2}{\partial x^2} \left[\frac{\partial W}{\partial t} - V_f \sin\theta \right], \xrightarrow{\int_{A_f} \rho_f dA_f} \tag{17b}$$

$$\begin{aligned} \frac{\partial P}{\partial x}.A_f = {} & m_f \frac{\partial^2 U_1}{\partial t^2} + m_f U_f \frac{\partial^2 W_1}{\partial x \partial t} \sin\theta + m_f U_f \frac{\partial^2 U_1}{\partial x \partial t} + m_f U_f^2 \frac{\partial^2 W_1}{\partial x^2} \sin\theta + \\ & \mu A_f \frac{\partial^3 U_1}{\partial x^2 \partial t} + \mu A_f U_f \frac{\partial^3 W_1}{\partial x^3} \sin\theta - \mu A_f U_f \left(\frac{\partial^2 W_1}{\partial x^2} \right)^2 \cos\theta. \end{aligned} \tag{17c}$$

$$\begin{aligned} \frac{\partial P}{\partial z}.A_f = {} & +\mu A_f \frac{\partial^3 W_1}{\partial x^2 \partial t} + U_f \mu A_f \frac{\partial^3 W_1}{\partial x^3} \cos\theta + U_f \mu A_f \left(\frac{\partial^2 W_1}{\partial x^2} \right)^2 \sin\theta + \\ & m_f \frac{\partial^2 W_1}{\partial t^2} + m_f U_f \frac{\partial^2 W_1}{\partial x \partial t} \cos\theta + m_f U_f \frac{\partial^2 W_1}{\partial x \partial t} + m_f U_f^2 \frac{\partial^2 W_1}{\partial x^2} \cos\theta. \end{aligned} \tag{17d}$$

In above equations (Eqs. (17c) and (17d)), the effect of viscosity is demonstrated [28, 27].

The governing equations for the conventional fluid-structure interaction problems have been derived by the assumption of no-slip boundary conditions. Consider a fully developed flow for a Newtonian fluid with a constant pressure gradient irrespective to gravitational body force; the Navier–Stokes equations will be given as follow [8, 9, 29]:

$$\rho_f \frac{d\vec{V}}{dt} = -\nabla \vec{P} + \mu_e \nabla^2 \vec{V}, \tag{18}$$

The solution Navier-Stokes equations and applying boundary conditions for Eq. (19), the final equation for Knudsen number reaching [8-9]:

$$\mathrm{VCF}=\frac{\mathrm{V}_{\mathrm{ave\_slip}}}{\mathrm{V}_{\mathrm{ave,(no\_slip)}}}=\left(1+\alpha\mathrm{Kn}\right)\left(1+4\left(\frac{2\text{-}\sigma_{\mathrm{v}}}{\sigma_{\mathrm{v}}}\right)\left(\frac{\mathrm{Kn}}{1+\mathrm{Kn}}\right)\right). \tag{19}$$

It is just adequate to replace the $\mathrm{V}_{\mathrm{avg,slip}}$ by $\mathrm{V}_{\mathrm{avg,slip}}=\mathrm{VCF}\times\mathrm{V}_{\mathrm{avg,(no\text{-}slip)}}$, in the governing equations. Magnetic field effects and Lorentz force will satisfy in this study by respect to [15-17] that Lorentz force vector will drive as below:

$$\mathrm{f}_{\mathrm{x,lorentz}}=0, \tag{20}$$

$$f_{y,lorentz}=\eta H_x^2\left(\frac{\partial^2 U}{\partial x^2}+\frac{\partial^2 V}{\partial y^2}+\frac{\partial^2 W}{\partial y\partial z}\right)=0, \tag{21}$$

$$f_{z,lorentz}=\eta H_x^2\left(\frac{\partial^2 W}{\partial x^2}+\frac{\partial^2 W}{\partial y^2}+\frac{\partial^2 W}{\partial y\partial z}\right)=\eta H_x^2\left(\frac{\partial^2 W}{\partial x^2}\right). \tag{22}$$

Based on the Visco-Pasternak foundation, the effects of the surrounding medium on the upper and lower nano tube are considered as follows:

$$q^{(m)}=2K_w W^{(m)}-2G_p\nabla^2 W^{(m)}+2C\frac{\partial W^{(m)}}{\partial t}-K_w W^{(n)}+G_p\nabla^2 W^{(n)}-C\frac{\partial W^{(n)}}{\partial t}, \tag{23}$$

where m and n $\left(\mathrm{m}\neq\mathrm{n}=1,2\right)$ indicate number of nanotubes. Here $\mathrm{K_w},\mathrm{C}$ and $\mathrm{G_p}$ are spring, damper and shear modulus of elastic medium, respectively.

In nano structure such as nanotubes and nano plates, the ratio of surface to volume is high relating micro scale, therefore the surface effect should be considered. According to Fig. 1 some essential surface layer's geometric specifications can be investigated as follows [10, 12]:

$$\begin{cases} A^s=\oint_s dA^s \xleftrightarrow[S:\ Surface\ layers\ surrounding]{dA^s=R_{out}d\theta\ ,\ circular\ closed\ path} \int_0^{2\pi} R_{out}d\theta \Rightarrow A^s=2\pi\left(R_{out}+R_{in}\right), \\ I^s=\oint_s z^2 dA^s \xleftrightarrow[(circular\ closed\ path)]{z=R_{out\ or\ in}\ \sin(\theta),} \int_0^{2\pi} R^3_{out\ or\ in}\sin^2\left(\theta\right)d\theta \Rightarrow I^s=\pi\left(R^3_{out}+R^3_{in}\right), \end{cases} \tag{24}$$

where R_i and R_o are the inner and outer radius of the CNT, respectively. To consider the surface stresses into structure, Gurtin and Murdoch [11] obtained theoretical relations based on the continuum mechanics including surface stress [11-12]. Based on this type of continuum elasticity theory, the surface is simulated as a mathematical layer of zero thickness with different material properties. They proposed the following general and simple expression for surface stress–strain relation in inner and outer CNT's layers for nonlinear EBB [12]:

$$\tau_{xx}^{Surf}=\tau^s-\frac{\tau^s}{2}\left(\frac{\partial W}{\partial x}\right)^2+\underbrace{\left(\lambda^s+2\mu^s\right)}_{E^s t^s}\left(\frac{\partial U}{\partial x}-z\frac{\partial^2 W}{\partial x^2}+\frac{1}{2}\left(\frac{\partial W}{\partial x}\right)^2\right), \tag{25}$$

where λ^s, μ^s and τ^s are surface Lame constants and residual surface stress respectively. Therefore, according to above relation and Hamilton's principal, motion equations are obtained for each nanotubes as follow:

$\delta U^{(m)}$:

$$-\frac{\partial N_{x(m)}^{Nonlocal}}{\partial x}+(m^{(m)}+m_f)\frac{\partial^2 U^{(m)}}{\partial t^2}+V_f m_f\frac{\partial^2 W^{(m)}}{\partial x\partial t}\sin\theta+m_f V_f^2\frac{\partial^2 W^{(m)}}{\partial x^2}\sin\theta= \\ \mu A_f\frac{\partial^3 U^{(m)}}{\partial x^2\partial t}+\mu A_f V_f\frac{\partial^3 W^{(m)}}{\partial x^3}\sin\theta-\mu A_f V_f(\frac{\partial^2 W^{(m)}}{\partial x^2})^2\cos\theta. \tag{26}$$

$\delta W^{(m)}$:

$$-\frac{\partial N_{x(m)}^{Nonlocal}}{\partial x}\frac{\partial W^{(m)}}{\partial x}-N_{x(m)}^{NL}\frac{\partial^2 W^{(m)}}{\partial x^2}-\frac{\partial^2 M_{x(m)}^{Nonlocal}}{\partial x^2}-\rho_t I_t^{(m)}\frac{\partial^4 W^{(m)}}{\partial x^2\partial t^2}+ \\ \left(m_f+m^{(m)}\right)\frac{\partial^2 W^{(m)}}{\partial t^2}+2V_f m_f\frac{\partial^2 W^{(m)}}{\partial x\partial t}\cos\theta+V_f m_f\frac{\partial^2 W^{(m)}}{\partial x^2}\frac{\partial W^{(m)}}{\partial t}\sin\theta- \\ V_f m_f\frac{\partial^2 W^{(m)}}{\partial x^2}\frac{\partial U^{(m)}}{\partial t}\cos\theta+V_f m_f\frac{\partial^2 W^{(m)}}{\partial x\partial t}\sin\theta-\rho_f I_f\frac{\partial^4 W^{(m)}}{\partial x^2\partial t^2}+m_f V_f^2\frac{\partial^2 W^{(m)}}{\partial x^2}\cos\theta- \\ q^{(m)}-\eta_m H_X^2(\frac{\partial^2 W^{(m)}}{\partial x^2})=\mu V_f A_f\frac{\partial^3 W^{(m)}}{\partial x^3}\cos\theta+\mu V_f A_f\left(\frac{\partial^2 W^{(m)}}{\partial x^2}\right)^2\sin\theta+\mu A_f\frac{\partial^3 W^{(m)}}{\partial x^2\partial t}. \tag{27}$$

Using Eq. (10) and (5) can be written as:

$$\begin{cases} \sigma_{xx}^{Nonlocal}-(e_0 a)^2\dfrac{\partial^2\sigma_{xx}^{Nonlocal}}{\partial x^2}=\overbrace{\tau_{xx}^{Bulk}+\tau_{xx}^{Surface}}^{\tau_{xx}} \\ \tau_{xx}^{Bulk}=E^*\left(\dfrac{\partial U}{\partial x}-z\dfrac{\partial^2 W}{\partial x^2}+\dfrac{1}{2}\left(\dfrac{\partial W}{\partial x}\right)^2\right)\xrightarrow[\int_A z\,dA=0,\ \int_A z^2 dA=I]{\int_A dA,\ E^*=E\left(1+g\left(\frac{\partial}{\partial u}\right)\right)} \\ \tau_{xx}^{Surface}=\underbrace{\left(\lambda^s+2\mu^s\right)}_{E^s t^s}\left(\dfrac{\partial U}{\partial x}-z\dfrac{\partial^2 W}{\partial x^2}+\dfrac{1}{2}\left(\dfrac{\partial W}{\partial x}\right)^2\right)+\tau^s-\dfrac{\tau^s}{2}\left(\dfrac{\partial W}{\partial x}\right)^2\xrightarrow[\oint_S z^2 dA^S=I^S]{\oint_S dA^S=A^S} \end{cases}, \tag{28a}$$

$$N_x^{Nonlocal}-(e_0 a)^2\frac{\partial^2 N_x^{Nonlocal}}{\partial x^2}=\left(E^*A+E^s t^s A^s\right)\left(\frac{\partial U}{\partial x}+\frac{1}{2}\left(\frac{\partial W}{\partial x}\right)^2\right)+\left(\tau^s-\frac{\tau^s}{2}\left(\frac{\partial W}{\partial x}\right)^2\right)A^s, \tag{28b}$$

$$M_x^{Nonlocal}-(e_0 a)^2\frac{\partial^2 M_x^{Nonlocal}}{\partial x^2}=-\left(E^*I+E^s I^s\right)\frac{\partial^2 W}{\partial x^2}. \tag{28c}$$

Using Eqs. (26-28) and use some mathematical manipulations the motion equations of coupled CNT system will be derived that mentioned in Appendix A.

Dimensionless parameters are defined as follows [27]:

$$(w_i,u_i)=\frac{(W_i,U_i)}{R_{out}},\quad \tau=\frac{t}{l}\sqrt{\frac{E}{\rho_t}},\quad \zeta=\frac{x}{l},\quad g^*=\frac{g}{l}\sqrt{\frac{E}{\rho_t}},$$

$$\bar{I}_i=\frac{\rho I_i}{\rho A_i R_{out}^2},\quad u_f=\sqrt{\frac{\rho_f}{E}}U_f,\quad \bar{\mu}=\frac{\mu}{R_{out}\sqrt{E\rho_f}},\quad \bar{\rho}=\frac{\rho_f}{\rho_t},$$

$$K_w=\frac{k_w l^2}{EA},\quad C_d=\frac{Cl}{EA}\sqrt{\frac{E}{\rho}},\quad K_g=\frac{G_p}{EA},\quad e_n=\frac{e_0 a}{l},$$

$$\bar{h}_1=\frac{E^s t^s I^s}{EAR_{out}^2},\quad \bar{\Pi}_0=\frac{\tau^s A^s}{\pi^2 EA},\quad \bar{h}_2=\frac{E^s t^s A^s}{EA},$$

$$H_x^*=\sqrt{\frac{\eta_m H_x^2}{EA}},\quad f=\frac{A_f}{A},\quad \eta=\frac{l}{R_{out}}.$$

Equations of motion will be converted to dimensionless form by using above dimensionless parameters.

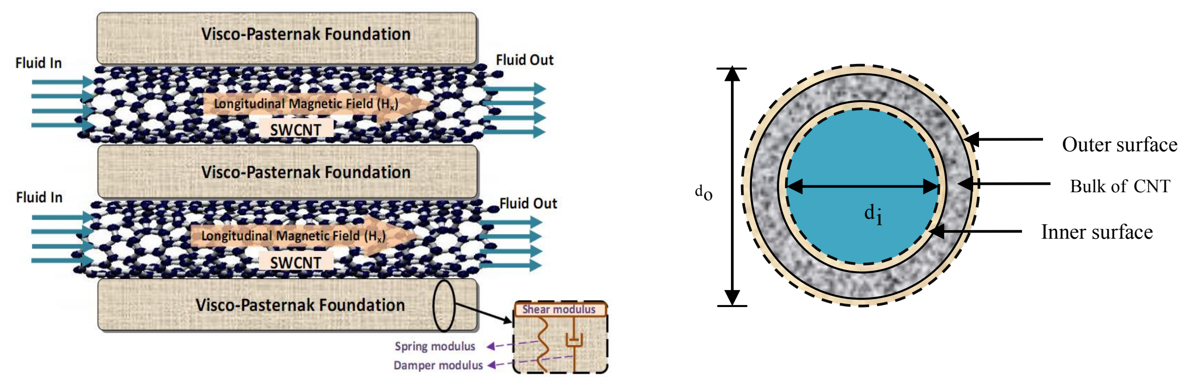

Fig. 1
Schematic of coupled CNTs conveying fluid under longitudinal magnetic field.

3 SOLUTION PROCEDURE

DQ method is a rather efficient numerical method for the solution of linear and nonlinear partial differential equations involving one dimension or multiple dimensions [32, 33]. A striking merit of the method is of high efficiency in computing complex nonlinear problems [34, 35], Compared with the standard numerical techniques such as the finite element and finite difference methods, the DQ method produces nonlinearity solution of reasonable accuracy with relatively small computational effort [36, 37]. The traditional linear algebraic approach, which is very successful for linear numerical computations, has been extended to handle the nonlinear problems. However, nonlinear problems have actually different from linear ones, linear algebraic and the relative matrix approaches, which are based on the concept of linear transformation. The Hadamard and SJT product of matrices are two types of special matrix product, They are alternate matrix approach to handle nonlinear problems [38].

To solve nonlinear equations by using DQ method, at first eliminating all the nonlinear terms in the matrices and calculating linear eigenvalues and eigenvectors. Then By using the Hadamard and SJT products, the nonlinear formulations are greatly simplified.

3.1 Hadamard product

Hadamard product of matrices and state its some properties first [39]. Based on the Hadamard product concept, the Hadamard power and function are also defined [39-38].

Let matrices $A=\left[a_{ij}\right]$ and $B=\left[b_{ij}\right]\in C^{N\times M}$ so $A\circ B=\left[a_{ij}b_{ij}\right]\in C^{N\times M}$, where $C^{N\times M}$ denotes the set of $\left(N\times M\right)$ real matrices and symbol *'o'* denotes Hadamard products.

3.2 SJT product

Chen [38] presented a new multiplication operation−SJT product of matrix and vector. If matrices $A=\left[a_{ij}\right]\in C^{N\times M}$, vector $B=\left[b_{ij}\right]\in C^{N\times 1}$, then $A\Diamond B=\left[a_{ij}b_{j}\right]\in C^{N\times M}$ $C^{N\times M}$, is defined as the post multiplying SJT product of matrix *A* and vector *B*, where '$\Diamond$' represented the SJT product.

3.3 Linear DQ procedure

DQ according to a spatial variable, a weighted linear combination of function values at some intermediate points in that variable is used. For example, the n^{th} order partial derivative of a function $g(x)$ at the i^{th} discrete point is approximated [40]:

$$g(x)=\frac{L(x)}{(x-x_i)L_i(x_i)} \qquad i=1,2,...,N, \tag{29}$$

$$L(x)=\prod_{j=1}^{N}(x-x_j), \qquad L_i(x)=\prod_{j=1}^{N}(x_i-x_j). \tag{30}$$

The weighting coefficient for the first order derivative is explicitly defined by:

$$C_{ij}^{(1)}=\frac{L_1(x_i)}{(x_i-x_j)L_1(x_j)} \qquad \text{for} \quad i\neq j, \quad i,j=1,2,...,N, \tag{31}$$

where x_i are the coordinates of the grid points in this work, the non-uniform grid distribution given by the Chebyshev points are used to calculate the weighting matrices and is given by [40, 41]:

$$\begin{gathered}X_i=\frac{L}{2}\left[1-\cos\left(\frac{i-1}{N-1}\right)\pi\right] \qquad i=1,...,N. \\ C^{(n)}=C^n \\ \frac{\partial^n w}{\partial\zeta^n}=\sum_{k=1}^{N}C_{ik}^{(n)}w_k \qquad i=1,....,N\end{gathered} \tag{32}$$

The solution of the motion equations that have been added to Appendix A can be assumed as follows [42, 43]:

$$u(x,\tau)=\bar{u}(x)e^{i\varpi\tau}, \qquad w(x,\tau)=\bar{w}(x)e^{i\varpi\tau}. \tag{33}$$

The DQ numerical solution approach equations of motion of coupled CNTs in dimensionless form as:

$$\delta u^{(m)}=0:\begin{cases}-\sum_{k=1}^{n}C_{ik}^{(2)}u_k^{(m)}-(1+\bar{\rho}f_m)\varpi^2u_k^{(m)}+e_n^2(1+\bar{\rho}f_m)\varpi^2\sum_{k=1}^{n}C_{ik}^{(2)}u_k^{(m)}-\bar{\mu}\sqrt{\bar{\rho}}f_m\frac{1}{\eta_m}(i\varpi)\sum_{k=1}^{n}C_{ik}^{(2)}u_k^{(m)} \\ +e_n^2\sqrt{\bar{\rho}}\bar{\mu}f_m\frac{1}{\eta_m}(i\varpi)\sum_{k=1}^{n}C_{ik}^{(4)}u_k^{(m)}=0.\end{cases} \tag{34}$$

$$\delta w^{(m)}=0:\begin{cases}\overline{\Delta T}\sum_{k=1}^{n}C_{ik}^{(2)}w_k^{(m)}-e_n^2\overline{\Delta T}\sum_{k=1}^{n}C_{ik}^{(4)}w_k^{(m)}+\bar{I}_m\left(\frac{1}{\eta_m}\right)^2\sum_{k=1}^{n}C_{ik}^{(4)}w_k^{(m)}+\bar{I}_m g^*\left(\frac{1}{\eta_m}\right)^2(i\varpi)\sum_{k=1}^{n}C_{ik}^{(4)}w_k^{(m)}\\+\left(\frac{1}{\eta_m}\right)^2\bar{I}_m\varpi^2\sum_{i=1}^{n}C_{ik}^{(2)}w_k^{(m)}+\overline{\Delta T}g^*(i\varpi)\sum_{k=1}^{n}C_{ik}^{(2)}w_k^{(m)}-\overline{\Delta T}e_n^2g^*(i\varpi)\sum_{k=1}^{n}C_{ik}^{(4)}w_k^{(m)}\\-e_n^2\bar{I}_m\left(\frac{1}{\eta_m}\right)^2\varpi^2\sum_{k=1}^{n}C_{ik}^{(4)}w_k^{(m)}-\left(1+f_m\bar{\rho}\right)\varpi^2w_k^{(m)}+\left(1+f_m\bar{\rho}\right)e_n^2\varpi^2\sum_{k=1}^{n}C_{ik}^{(2)}w_k^{(m)}\\+2\sqrt{\bar{\rho}}f_mu_f(i\varpi)\sum_{k=1}^{n}C_{ik}^{(1)}w_k^{(m)}-2e_n^2\sqrt{\bar{\rho}}f_mu_f(i\varpi)\sum_{k=1}^{n}C_{ik}^{(3)}w_k^{(m)}+\bar{\rho}f_m\bar{I}_f\left(\frac{1}{\eta_m}\right)^2\varpi^2\sum_{k=1}^{n}C_{ik}^{(2)}w_k^{(m)}\\+\bar{\rho}f_me_n^2\bar{I}_f\left(\frac{1}{\eta_m}\right)^2\sum_{k=1}^{n}C_{ik}^{(4)}w_k^{(m)}+f_mu_f^2\sum_{k=1}^{n}C_{ik}^{(2)}w_k^{(m)}-f_mu_f^2e_n^2\sum_{k=1}^{n}C_{ik}^{(4)}w_k^{(m)}\\-\sqrt{\bar{\rho}}f_m\bar{\mu}\frac{1}{\eta_m}(i\varpi)\sum_{k=1}^{n}C_{ik}^{(2)}w_k^{(m)}+e_n^2\sqrt{\bar{\rho}}f_m\bar{\mu}\frac{1}{\eta_m}(i\varpi)\sum_{k=1}^{n}C_{ik}^{(4)}w_k^{(m)}-f_m\bar{\mu}u_f\left(\frac{1}{\eta_m}\right)\sum_{k=1}^{n}C_{ik}^{(3)}w_k^{(m)}\\+f_me_n^2\bar{\mu}u_f\left(\frac{1}{\eta_m}\right)\sum_{i=1}^{n}C_{ik}^{(5)}w_k^{(m)}+\bar{h}\left(\frac{1}{\eta_m}\right)^2\bar{I}_m\sum_{i=1}^{n}C_{ik}^{(4)}w_k^{(m)}-H_x^*\sum_{k=1}^{n}C_{ik}^{(2)}w_k^{(m)}\\+H_x^*e_n^2\sum_{k=1}^{n}C_{ik}^{(4)}w_k^{(m)}-\bar{\Pi}_0\sum_{k=1}^{n}C_{ik}^{(2)}w_k^{(m)}+e_n^2\bar{\Pi}_0\sum_{k=1}^{n}C_{ik}^{(4)}w_k^{(m)}+2K_ww_k^{(m)}-2K_we_n^2\sum_{k=1}^{n}C_{ik}^{(2)}w_k^{(m)}\\-K_ww_k^{(j)}+K_we_n^2\sum_{k=1}^{n}C_{ik}^{(2)}w_k^{(j)}+2C_d(i\omega)w_k^{(m)}-2C_d(i\omega)e_n^2\sum_{k=1}^{n}C_{ik}^{(2)}w_k^{(m)}-C_d(i\omega)w_k^{(j)}\\+C_de_n^2\omega\sum_{k=1}^{n}C_{ik}^{(2)}w_k^{(j)}-2K_g\sum_{k=1}^{n}C_{ik}^{(2)}w_k^{(m)}+2K_ge_n^2\sum_{k=1}^{n}C_{ik}^{(4)}w_k^{(m)}+K_g\sum_{k=1}^{n}C_{ik}^{(2)}w_k^{(j)}\\-K_ge_n^2\sum_{k=1}^{n}C_{ik}^{(4)}w_k^{(j)}=0.\end{cases}\tag{35}$$

where $\varpi=\omega h\sqrt{\rho_f/E}$ the dimensionless natural frequency, ω is natural frequency and ρ_f is density of fluid. Also the DQ approach form of mechanical linear boundary conditions at both ends in each layer of elastic coupled CNT may be written in dimensionless form as:

$$\underbrace{\begin{matrix}w_{i=1}=v_{i=1}=u_{i=1}=0\\w_{i=N}=v_{i=N}=u_{i=N}=0\end{matrix}}_{\text{Geometric }\textit{boundary condition}}\quad\&\quad\underbrace{\begin{matrix}\frac{\partial w}{\partial\zeta}=\sum_{j=1}^{N}C_{2j}^{(1)}w_j^{(m)}=0\\\frac{\partial w}{\partial\zeta}=\sum_{j=1}^{N}C_{(N-1)j}^{(1)}w_j^{(m)}=0\end{matrix}}_{\text{Geometric }\textit{boundary condition}}\qquad \textit{for Clamped}\ \&\ i=1\ldots N.\tag{36}$$

$$\underbrace{\begin{matrix}w_{i=1}=v_{i=1}=u_{i=1}=0\\w_{i=N}=v_{i=N}=u_{i=N}=0\end{matrix}}_{\text{Geometric B.C.}}\ \&\ \underbrace{\begin{matrix}\mathrm{M}_{xx}\big|_{\text{first}}=0\Rightarrow\left(EI+E^sI^s\right)\frac{\partial^2w}{\partial\zeta^2}=\left(EI+E^sI^s\right)\sum_{j=1}^{N}C_{2j}^{(2)}w_j^{(m)}=0\\\mathrm{M}_{xx}\big|_{\text{end}}=0\Rightarrow\left(EI+E^sI^s\right)\frac{\partial^2w}{\partial\zeta^2}=\left(EI+E^sI^s\right)\sum_{j=1}^{N}C_{(N-1)j}^{(2)}w_j^{(m)}=0\end{matrix}}_{\text{Geometric B.C.}}\quad \begin{matrix}\text{for Pined}\\ \text{i=1...N}\end{matrix}\tag{37}$$

Eqs. (36-37) named boundary condition equations and Eqs. (34-35) are domain equation. Linear differential boundary condition and linear differential equation of motion will be changed to algebraic equations by DQ approach. Eqs. (34-37) lead the following constitutive matrix equation as:

$$\left(-\underbrace{\begin{bmatrix}[M_{bb}]=[0] & [M_{bd}]=[0]\\ [M_{db}] & [M_{dd}]\end{bmatrix}}_{[M]}\varpi^2+\underbrace{\begin{bmatrix}[D_{bb}]=[0] & [D_{bd}]=[0]\\ [D_{db}] & [D_{dd}]\end{bmatrix}}_{[D]}(i\varpi)+\underbrace{\begin{bmatrix}[K_{bb}] & [K_{bd}]\\ [K_{db}] & [K_{dd}]\end{bmatrix}}_{[K]}\right)\begin{Bmatrix}d_b\\ d_d\end{Bmatrix}=0. \tag{38}$$

$$\{d\}=\left\{\{u_1^1 u_2^1 \ldots u_{N-1}^1 u_N^1\}\{w_1^1 w_2^1 w_3^1 \ldots w_{N-2}^1 w_{N-1}^1 w_N^1\}\{u_1^2 u_2^2 \ldots u_{N-1}^2 u_N^2\}\{w_1^2 w_2^2 w_3^2 \ldots w_{N-2}^2 w_{N-1}^2 w_N^2\}\right\}^T.$$

where $[K],[D]$ and $[M]$ are the stiffness matrix, damping matrix and mass matrix, respectively, and subscript *b* denotes the elements related to the boundary points while subscript *d* is associated with the remainder elements. Eq. (38) can be expressed as below:

$$\begin{aligned}&[K_{bb}]\{d_b\}+[K_{bd}]\{d_d\}=0 \quad \Rightarrow \{d_b\}=-[K_{bb}]^{-1}[K_{bd}]\{d_d\},\\ &-[M_{db}]\varpi^2\{d_b\}-[M_{dd}]\varpi^2\{d_d\}+[D_{db}](i\varpi)\{d_b\}+[D_{dd}](i\varpi)\{d_d\}+[K_{db}]\{d_b\}+[K_{dd}]\{d_d\}=0\ ,\end{aligned} \tag{39}$$

Using Eq. (39), equation of motion can be written as:

$$-[M_e]\varpi^2\{d_d\}+[D_e](i\varpi)\{d_d\}+[K_e]\{d_d\}=0. \tag{40}$$

That M_e, D_e and K_e are the primary mass, damper and stiffness finally matrices which have been written as follows:

$$\begin{aligned}&[M_e]=[M_{dd}]-[M_{db}]\left([K_{bb}]^{-1}[K_{bd}]\right)\\ &[D_e]=[D_{dd}]-[D_{db}]\left([K_{bb}]^{-1}[K_{bd}]\right)\\ &[K_e]=[K_{dd}]-[K_{db}]\left([K_{bb}]^{-1}[K_{bd}]\right).\end{aligned} \tag{41}$$

For solving the Eq. (40) and reducing it to the standard form of eigenvalues problem, it is convenient to rewrite Eq. (41) as the following first order variable as:

$$\begin{cases}\left(-[M_e]\varpi^2+[D_e](i\varpi)+[K_e]\right)\{d_d\}=0\\ (\varpi)\{d_d\}=\{d^*\}\end{cases} \Rightarrow \begin{cases}-[M_e]\varpi\{d^*\}+i[D_e]\{d^*\}+[K_e]\{d_d\}=0\\ \varpi\{d_d\}=\{d^*\}\end{cases}$$

$$\Rightarrow\left(\underbrace{\begin{bmatrix}[0]_{(n-8)\times(n-8)} & [I]_{(n-8)\times(n-8)}\\ [M_e]^{-1}_{(n-8)\times(n-8)}[K_e]_{(n-8)\times(n-8)} & i[M_e]^{-1}_{(n-8)\times(n-8)}[D_e]_{(n-8)\times(n-8)}\end{bmatrix}}_{[A]_{(2(n-8))\times(2(n-8))}}-\varpi[I]_{(2(n-8))\times(2(n-8))}\right)\begin{Bmatrix}d_d\\ d^*\end{Bmatrix}=0. \tag{42}$$

where $[A],[0]$ and $[I]$ are the state, zero and unitary matrices, respectively. The solution of Eq. (42) is complex due to the presence of fluid flow viscous damping. Hence, the results are containing two real and imaginary parts. The imaginary part is corresponding to the system damping and the real part representing natural frequencies of the system.

3.4 Non-linear DQ procedure

The nonlinear DQ numerical solution approach equations of motion of coupled CNT in dimensionless form are shown at Appendix A. using Hadamard and SJT operators, the nonlinear terms of Eqs. (A1-A2) are simplified. To solve nonlinear equation by DQ method has some steps that are:

1. Scaling up the linear eigenvectors and using, Hadamard, SJT products and linear eigenvectors to estimate nonlinear terms of Eqs. (A.1-A.2).

2. Adding nonlinear matrices to linear matrices and calculating eigenvalues and eigenvectors of the updated eigenvalues problem.

$$\left(-\underbrace{\begin{bmatrix}[M_{bb}]=[0] & [M_{bd}]=[0]\\ [M_{db}] & [M_{dd}]\end{bmatrix}}_{[M]}\varpi^2+\underbrace{\begin{bmatrix}[D_{bb}]=[0] & [D_{bd}]=[0]\\ [D_{db}] & [D_{dd}]\end{bmatrix}}_{[D]}(i\varpi)+\underbrace{\begin{bmatrix}[K_{bb}] & [K_{bd}]\\ [K_{db}] & [K_{dd}]\end{bmatrix}}_{[K]}\right)\begin{Bmatrix}d_b\\ d_d\end{Bmatrix}=0,$$

$$[M]=[M_L+M_{NL}],[D]=[D_L+D_{NL}],[K]=[K_L+K_{NL}].$$

Natural frequency of nonlinear equations will obtain like Eqs. (34) to (35) in prior section.

3. Repeat step (2) until the response converges to a prescribed error tolerance

$$\text{Error}=\sqrt{\sum\left(\varpi_{NL}^{(k)}-\varpi_L\right)^2/\sum\left(\varpi_{NL}^{(k+1)}\right)^2}\le\sqrt{10^{-3}\text{ or }10^{-4}}$$

4 NUMERICAL RESULTS AND DISCUSSION

In this study, nonlinear vibration of coupled CNTs system conveying fluid linked by visco-Pasternak medium is carried out. In following figures the effects of parameters such small scale, elastic medium, Knudsen number, visco-elastic structural damping coefficient and magnetic field on frequency versus fluid velocity (U_f) of the clamp-clamp coupled CNTs are discussed in detail. It is noted that $\text{Re}(\varpi)$ represents the resonance frequencies of the coupled CNTs while $\text{Im}(\varpi)$ denotes the damping which resulting from the moving fluid to the CNTs. Mechanical and geometrical properties of the CNTs are considered as [44, 10]:

$E=1TPa$	$k_w=10^9\ \frac{N}{m^2}$	$E^s t^s=5.1882\ \frac{N}{m}$
$r_i=3.54nm$	$\mu=0.635\times10^{-3}\ \frac{Ns}{m}$	
$h=0.34\,nm$	$\rho_t=2.3\ \frac{gr}{cm^3}$	
$l=35.4nm$	$\tau^s=0.9108\ \frac{N}{m}$.	

In order to validate the accuracy of this study, Tables 1-3. show comparison the DQ result of this study with Galerkin method [43] for different boundary conditions. A simplified case of the analysis is carried out by considering CNTs conveying fluid and neglecting viscoelastic characteristics, Knudsen number, surface effect and magnetic field effects. The dimensionless natural and damping frequencies versus the dimensionless flow velocity (u_f) for different vibration mode are depicted in Figs. 2(a) and 2(b), respectively. Generally, the system is stable when the imaginary part of the frequency remains zero and it is unstable when the imaginary and real parts of the frequency become positive and zero, respectively. It can be seen that $\text{Re}(\varpi)$ decreases with increasing u_f.As the dimensionless flow velocity increases at the vicinity of 0.229, both $\mathrm{Im}(\varpi)$ and $\mathrm{Re}(\varpi)$ are equal to zero for the first mode. In this region, the coupled system becomes unstable and susceptible to buckling due to the divergence via a pitchfork bifurcation. The corresponding fluid velocity is called the critical flow velocity. For $0.229<u_f<0.326$ and $e_0a=0$ nm the real part of first mode is exactly zero while the imaginary part becomes nonzero. When the flow velocity increases beyond 0.336, the coupled system undergoes a flutter. As the flow velocity reaches about 0.326, the CNTs system regains stability in the first mode. By increasing the flow velocity the sequence of the divergence, flutter and stable behaviors is occurred again. The same behavior can also be observed for other vibration modes. Fig. 3 shows the difference between linear and nonlinear solutions for clamped ends boundary condition. It is visible in this figure that the nonlinear geometric terms play stabilizer role for the structure. This effect will grow when the dimensionless fluid flow velocity go over of $u_f=0.087$ the effects of nonlinear geometrics terms become undeniable. Fig. 4 shows real part of dimensionless frequency versus flow velocity for different values of dimensionless small scale parameter. Also in this figure demonstrates the nonlinear frequency for $e_0a=1.2\mathrm{nm}$. It is obvious that nonlocal parameter is a significant parameter in vibration of coupled system. As can be seen increasing the nonlocal parameter decreases the frequency and critical flow velocity. This decrease can be attributed to the distributed transverse force due to the curvature change in the nano structure and the interaction between the atom at reference point and all other atoms. It is need to point out that, the zero value for nonlocal parameter (i.e. $e_0a=0$) denotes the result obtained by the classical EBB model which has the highest frequency and critical fluid velocity.

The effects of foundation stiffness on natural frequency are shown in Fig. 5. This figure demonstrates that the visco-Pasternak foundation has lowest stability where critical flow velocity is 0.171 and Pasternak foundation has largest stability. The effect of visco-elastic structural damping coefficient on dimensionless nonlinear natural frequency is shown in Fig. 6. It can be concluded that elastic CNTs ($g^*=0$) has the most value of critical fluid velocity and located at the top of other curves. Moreovere, increasing the visco-elastic structural damping coefficient, shifts the curves to the lower frequency zone.

Table1
Comparison of the frequency of the present work with those obtained by other methods for a CNT conveying fluid for clamped-clamped boundary condition

		Linear DQ Method (C-C)	Galerkin Method (C-C)	Nonlinear DQ Method (C-C)	Compare NL and LDQ's results
$K_w=0.0769$	$V_{fluid}=0.1$	$\omega=0.9845$	$\omega=0.9845$	$\omega=0.9908$	0.64%
	$V_{fluid}=0.15$	$\omega=0.8126$	$\omega=0.8126$	$\omega=0.8216$	1.1%
	$V_{fluid}=0.2$	$\omega=0.5313$	$\omega=0.5313$	$\omega=0.5448$	2.54%
	$(\omega=0)V_{fluid(CR)}$	0.238	0.238	0.241	1.26%
$K_w=0.1538$	$V_{fluid}=0.15$	$\omega=0.8326$	$\omega=0.8326$	$\omega=0.8413$	0.87%
	$V_{fluid}=0.2$	$\omega=0.5577$	$\omega=0.5577$	$\omega=0.5702$	1.25%
	$V_{fluid}=0.22$	$\omega=0.3933$	$\omega=0.3933$	$\omega=0.4121$	1.88%
	$(\omega=0)V_{fluid(CR)}$	0.242	0.242	0.244	0.2%
$K_w=0.2307$	$V_{fluid}=0.18$	$\omega=0.7065$	$\omega=0.7065$	$\omega=0.7155$	0.9%
	$V_{fluid}=0.2$	$\omega=0.5829$	$\omega=0.5829$	$\omega=0.5946$	1.17%
	$V_{fluid}=0.24$	$\omega=0.1775$	$\omega=0.1775$	$\omega=0.2175$	4%
	$(\omega=0)V_{fluid(CR)}$	0.245	0.245	0.247	0.81%

Table2
Comparison of the frequency of the present work with those obtained by other methods for a CNT conveying fluid for clamped-simply boundary condition

		Linear DQ Method (C-S)	Galerkin Method (C-S)	Nonlinear DQ Method(C-S)	Compare NL and LDQ's results
$K_w = 0.0769$	$V_{fluid} = 0.01$	$\omega = 0.5222$	$\omega = 0.5222$	$\omega = 0.4623$	12.95%
	$V_{fluid} = 0.05$	$\omega = 0.4792$	$\omega = 0.4792$	$\omega = 0.425$	12.75%
	$V_{fluid} = 0.1$	$\omega = 0.3208$	$\omega = 0.3208$	$\omega = 0.288$	11.38%
	$(\omega = 0) V_{fluid(CR)}$	0.13	0.13	0.13	0%
$K_w = 0.1538$	$V_{fluid} = 0.05$	$\omega = 0.5167$	$\omega = 0.5167$	$\omega = 0.469$	10.17%
	$V_{fluid} = 0.1$	$\omega = 0.3717$	$\omega = 0.3717$	$\omega = 0.3464$	7.31%
	$V_{fluid} = 0.13$	$\omega = 0.1775$	$\omega = 0.1775$	$\omega = 0.1868$	5.23%
	$(\omega = 0) V_{fluid(CR)}$	0.139	0.139	0.142	2.15%
$K_w = 0.2307$	$V_{fluid} = 0.01$	$\omega = 0.8266$	$\omega = 0.8266$	$\omega = 0.7796$	6.02%
	$V_{fluid} = 0.05$	$\omega = 0.7924$	$\omega = 0.7924$	$\omega = 0.7411$	6.92%
	$V_{fluid} = 0.14$	$\omega = 0.5145$	$\omega = 0.5145$	$\omega = 0.3705$	38.86%
	$(\omega = 0) V_{fluid(CR)}$	0.186	0.186	0.165	12.72%

Table3
Comparison of the frequency of the present work with those obtained by other methods for a CNT conveying fluid for simply-simply boundary condition.

		Linear DQ Method (S-S)	Galerkin Method (S-S)	Nonlinear DQ Method(S-S)	Compare NL and L DQ's results
$K_w = 0.0769$	$V_{fluid} = 0.01$	$\omega = 0.5222$	$\omega = 0.5222$	$\omega = 0.4623$	12.95%
	$V_{fluid} = 0.05$	$\omega = 0.4792$	$\omega = 0.4792$	$\omega = 0.425$	12.75%
	$V_{fluid} = 0.1$	$\omega = 0.3208$	$\omega = 0.3208$	$\omega = 0.288$	11.38%
	$(\omega = 0) V_{fluid(CR)}$	0.13	0.13	0.13	0%
$K_w = 0.1538$	$V_{fluid} = 0.05$	$\omega = 0.5167$	$\omega = 0.5167$	$\omega = 0.469$	10.17%
	$V_{fluid} = 0.1$	$\omega = 0.3717$	$\omega = 0.3717$	$\omega = 0.3464$	7.31%
	$V_{fluid} = 0.13$	$\omega = 0.1775$	$\omega = 0.1775$	$\omega = 0.1868$	5.23%
	$(\omega = 0) V_{fluid(CR)}$	0.139	0.139	0.142	2.15%
$K_w = 0.2307$	$V_{fluid} = 0.01$	$\omega = 0.5905$	$\omega = 0.5905$	$\omega = 0.5423$	8.88%
	$V_{fluid} = 0.05$	$\omega = 0.5517$	$\omega = 0.5517$	$\omega = 0.509$	8.54%
	$V_{fluid} = 0.14$	$\omega = 0.1596$	$\omega = 0.1596$	$\omega = 0.1994$	19.9%
	$(\omega = 0) V_{fluid(CR)}$	0.147	0.147	0.151	2.72%

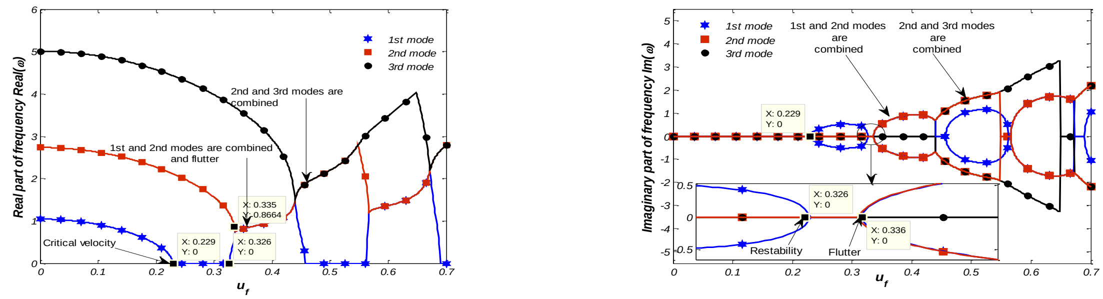

Fig. 2
a) Dimensionless natural frequencies versus dimensionless fluid velocity for clamped end boundary condition. b) Dimensionless damping frequencies versus dimensionless fluid velocity for clamped end boundary condition.

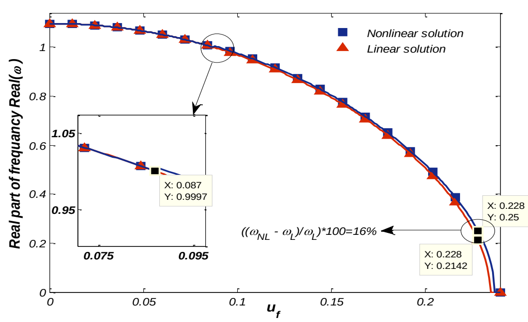

Fig. 3
Dimensionless natural frequencies versus dimensionless fluid velocity for linear and nonlinear solutions.

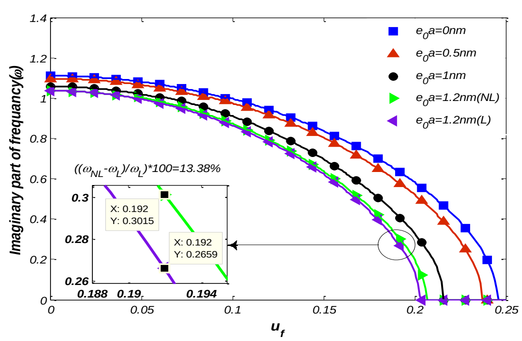

Fig. 4
Effect of small scale parameter on dimension natural frequency versus dimension flow velocity.

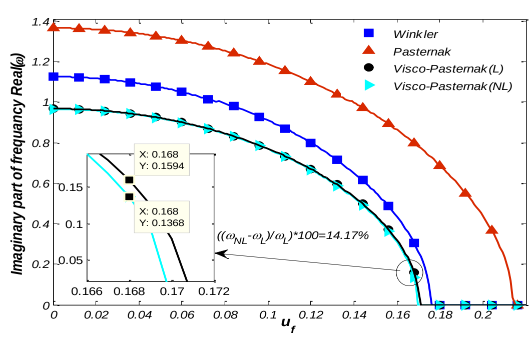

Fig. 5
Effect of the elastic foundation on the dimension natural frequency versus dimension flow velocity.

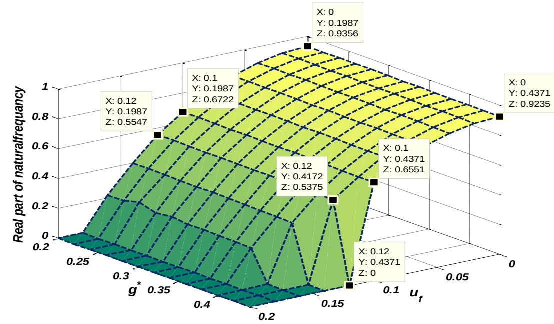

Fig. 6
Effect of the viscoelastic structural damping of CNTs on the dimensionless natural frequency.

Nonlinear variation of natural frequency with respect to fluid velocity for different values of Knudsen number is illustrated in Fig. 7. As already was mentioned, Knudsen number is defined based on various flow regimes where the slip flow regime is considered. As shown in these figures, continuum fluid ($Kn = 0$) predicts the highest frequency zone. Considering fluid with higher Knudsen number results in shifting the curves to the lower frequency region. Therefore critical flow velocity of coupled system decreases with increasing Knudsen number.

The effect of longitudinal magnetic field on nonlinear dimensionless frequency of coupled CNTs is shown in Fig. 8. As already was mentioned applying magnetic field in axial direction generate the force in radial direction which is called Lorentz force. It is concluded that frequency and critical flow velocity increase with increasing longitudinal magnetic intensity. This is due to the coupling effect of the vibrating double CNT and the longitudinal magnetic field. Regarding Lorentz force effect, it is evident that the longitudinal magnetic field is fundamentally an effective factor on increasing resonance frequency leading to stability of system. Figs. 9 and 10 depict the effect of surface stress effect on dimensionless frequency of coupled system. It is evident that surface stress plays an important role on natural frequency. The residual surface tension is $\left(\tau^s = 0.9108 \text{N/m}\right)$, Young's modules multiply thickness of both surface layers is $\left(E^s t^s = 5.1882 \text{N/m}\right)$ and aspect ratio is $\left(l/R_{out} = 20\right)$. The nonlinear frequency values and stability of the system in this study are higher than those obtained by Wang [10] with the lack of surface stress effect. It is found that by increasing bending rigidity and surface residual stress, CNT's stability will increase. Figs. 11 and 12 show the first and second flutter displacements where modes 1 and 2 and modes 2 and 3 are combined, respectively for pined- pined boundary condition.

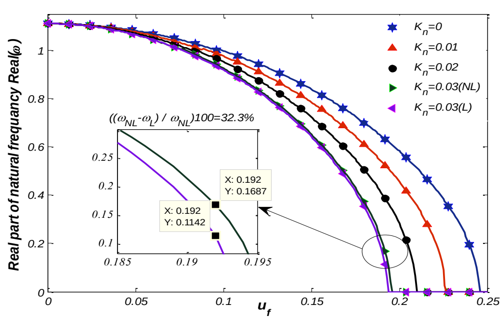

Fig. 7
Effect of Knudsen number on dimensionless natural frequency.

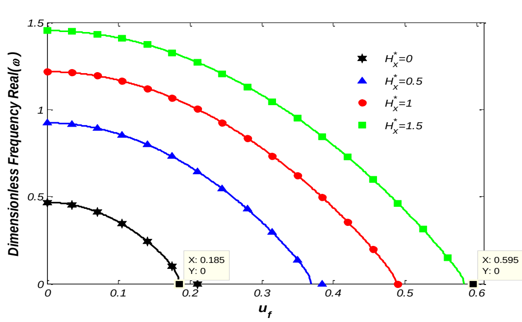

Fig. 8
Effect of longitudinal magnetic field on dimensionless frequency of double CNTs.

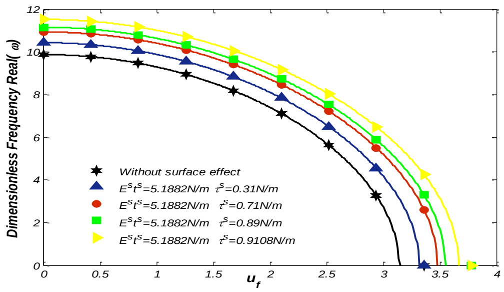

Fig. 9
Surface effect on dimensionless natural frequency.

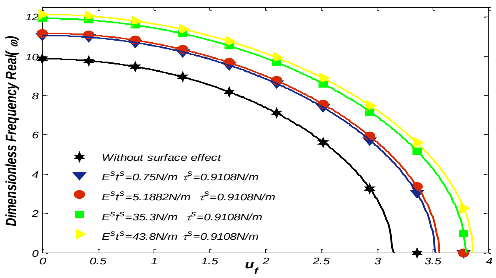

Fig. 10
Surface effect on dimensionless natural frequency.

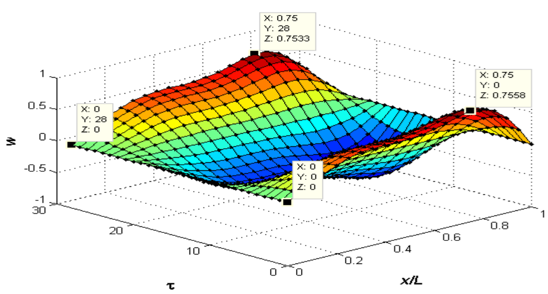

Fig. 11
The transverse displacement of the combination of modes 1 and 2 versus varieties of time.

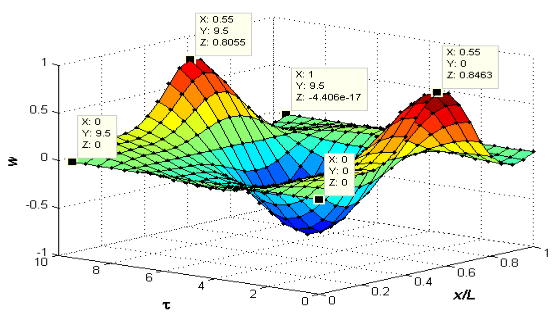

Fig. 12
The transverse displacement of the combination of modes 2 and 3 versus varieties of time.

5 CONCLUSIONS

In this work, nonlinear vibration of double bonded visco-CNTs conveying viscous fluid embedded in a visco-Pasternak medium was investigated. Coupled visco-elastic nano system is placed in a uniform longitudinal magnetic field and the surface stress effect was considered. The higher order governing equations of motion are solved by DQ approach in which Hamilton's principle was used to obtain fundamental governing equations. The results presented in this work can be useful for the study and design of the next generation of nano/micro structures that make use of the nonlocal vibration properties of visco CNTs embedded in visco-Pasternak medium. The following conclusions may be made from the results:

1. Regarding fluid flow effects, it has been concluded that the fluid flow is basically an effective factor on decreasing natural frequency leading to instability of the coupled nano system.

2. The stability of the coupled visco CNTs is strongly dependent on the imposed longitudinal magnetic field so that increasing the imposed longitudinal magnetic field significantly increases the stability of the system. In this case the stability of the system can be controlled by imposing longitudinal magnetic field and the coupled CNTs can behave as an actuator.

3. Increasing the small scale parameter decreases the real and real parts of frequency and critical fluid velocity.

4. Increase of damping constant of medium and visco-elastic parameter of CNTs caused to decrease of stability of visco coupled system.

5. The results of this study are validated as far as possible by another numerical analysis method (Galerkin method) at Table 1-3.

The result of this study can be used in design and optimization of nano-devices such as drug delivery systems and sensitive applications.

ACKNOWLEDGEMENTS

The author would like to thank the reviewers for their valuable comments and suggestions to improve the clarity of this study. The authors are grateful to University of Kashan for supporting this work by Grant No. 363443/17. They would also like to thank the Iranian Nanotechnology Development Committee for their financial support.

APPENDIX A

Nonlinear equations of CNT's motion respect to longitudinal direction can be simplified as below: $\delta U_{(m)}=0 \Rightarrow$

$$\begin{aligned}
&-\left(EA+E^s t^s A^s\right)\frac{\partial^2 U_{(m)}}{\partial x^2}+\left(EA+E^s t^s A^s\right)\frac{\partial^2 W_{(m)}}{\partial x^2}\frac{\partial W_{(m)}}{\partial x}+\tau^s A^s\frac{\partial W}{\partial x}\frac{\partial^2 W}{\partial x^2}V_f m_f\frac{\partial^2 W_{(m)}}{\partial x\partial t}\frac{\partial W_{(m)}}{\partial x}+\\
&(e_0a)^2 V_f m_f\frac{\partial^4 W_{(m)}}{\partial x^3\partial t}\frac{\partial W_{(m)}}{\partial x}+(e_0a)^2 V_f m_f\frac{\partial^2 W_{(m)}}{\partial x\partial t}\frac{\partial^3 W_{(m)}}{\partial x^3}-(e_0a)^2 V_f m_f\frac{\partial^2 W_{(m)}}{\partial x\partial t}\left(\frac{\partial^2 W_{(m)}}{\partial x^2}\right)^2\frac{\partial W_{(m)}}{\partial x}+\\
&2(e_0a)^2 V_f m_f\frac{\partial^3 W_{(m)}}{\partial x^2\partial t}\frac{\partial^2 W_{(m)}}{\partial x^2}-\mu A_f\frac{\partial^3 U_{(m)}}{\partial x^2\partial t^2}-(e_0a)^2\left(m_{(m)}+m_f\right)\frac{\partial^4 U_{(m)}}{\partial x^2\partial t^2}-m_f V_f^2\frac{\partial^2 W_{(m)}}{\partial x^2}\frac{\partial W_{(m)}}{\partial x}+\\
&(e_0a)^2 m_f V_f^2\frac{\partial^4 W_{(m)}}{\partial x^4}\frac{\partial W_{(m)}}{\partial x}+\left(m_{(m)}+m_f\right)\frac{\partial^2 U_{(m)}}{\partial t^2}-3(e_0a)^2 m_f V_f^2\frac{\partial^2 W_{(m)}}{\partial x^2}\frac{\partial^3 W_{(m)}}{\partial x^3}-\\
&(e_0a)^2 m_f V_f^2\left(\frac{\partial^2 W_{(m)}}{\partial x^2}\right)^3\frac{\partial W_{(m)}}{\partial x}+(e_0a)^2\mu A_f\frac{\partial^5 U_{(m)}}{\partial x^4\partial t}+\mu A_f V_f\frac{\partial^3 W_{(m)}}{\partial x^3}\frac{\partial W_{(m)}}{\partial x}-\\
&(e_0a)^2\mu A_f V_f\left(\frac{\partial^3 W_{(m)}}{\partial x^3}\right)^2-(e_0a)^2\mu A_f V_f\frac{\partial^5 W_{(m)}}{\partial x^5}\frac{\partial W_{(m)}}{\partial x}+(e_0a)^2\mu A_f V_f\frac{\partial^3 W_{(m)}}{\partial x^3}\left(\frac{\partial^2 W_{(m)}}{\partial x^2}\right)^2\frac{\partial W_{(m)}}{\partial x}-\\
&2(e_0a)^2\mu A_f U_f\frac{\partial^4 W_{(m)}}{\partial x^4}\frac{\partial^2 W_{(m)}}{\partial x^2}+\mu A_f U_f\left(\frac{\partial^2 W_{(m)}}{\partial x^2}\right)^2-2(e_0a)^2\mu A_f U_f\frac{\partial^4 W_{(m)}}{\partial x^4}\frac{\partial^2 W_{(m)}}{\partial x^2}-\\
&2(e_0a)^2\mu A_f U_f\left(\frac{\partial^3 W_{(m)}}{\partial x^3}\right)^2+(e_0a)^2\mu A_f U_f\left(\frac{\partial^2 W_{(m)}}{\partial x^2}\right)^4+5(e_0a)^2\mu A_f U_f\frac{\partial^3 W_{(m)}}{\partial x^3}\left(\frac{\partial^2 W_{(m)}}{\partial x^2}\right)^2\frac{\partial W_{(m)}}{\partial x}=0.
\end{aligned} \tag{A.1}$$

Nonlinear equations of CNT's motion respect to transverse direction can be simplified as below: $\delta W_{(m)}=0 \Rightarrow$

$$
\begin{aligned}
&(e_0a)^2\left(EA+E^st^sA^s\right)\left(\frac{3}{2}\frac{\partial^4 W_{(m)}}{\partial x^4}\left(\frac{\partial W_{(m)}}{\partial x}\right)^2+9\frac{\partial W_{(m)}}{\partial x}\frac{\partial^2 W_{(m)}}{\partial x^2}\frac{\partial^3 W_{(m)}}{\partial x^3}+3\left(\frac{\partial^2 W_{(m)}}{\partial x^2}\right)^3\right)+\\
&(e_0a)^2\left(EA+E^st^sA^s\right)\left(3\frac{\partial^3 U_{(m)}}{\partial x^3}\frac{\partial^2 W_{(m)}}{\partial x^2}+3\frac{\partial^2 U_{(m)}}{\partial x^2}\frac{\partial^3 W_{(m)}}{\partial x^3}+\frac{\partial^4 U_{(m)}}{\partial x^4}\frac{\partial W_{(m)}}{\partial x}+\frac{\partial U_{(m)}}{\partial x}\frac{\partial^4 W_{(m)}}{\partial x^4}\right)+\\
&(e_0a)^2\,EAg\left(2\frac{\partial W_{(m)}}{\partial x}\frac{\partial^4 W_{(m)}}{\partial x^4}\frac{\partial^2 W_{(m)}}{\partial x\partial t}+6\frac{\partial W_{(m)}}{\partial x}\frac{\partial^3 W_{(m)}}{\partial x^3}\frac{\partial^3 W_{(m)}}{\partial x^2\partial t}+6\frac{\partial W_{(m)}}{\partial x}\frac{\partial^2 W_{(m)}}{\partial x^2}\frac{\partial^4 W_{(m)}}{\partial x^3\partial t}\right)+\\
&(e_0a)^2\,EAg\left(\left(\frac{\partial W_{(m)}}{\partial x}\right)^2\frac{\partial^5 W_{(m)}}{\partial x^4\partial t}+6\frac{\partial^2 W_{(m)}}{\partial x^2}\frac{\partial^3 W_{(m)}}{\partial x^3}\frac{\partial^2 W_{(m)}}{\partial x\partial t}+\frac{\partial W_{(m)}}{\partial x}\frac{\partial^5 U_{(m)}}{\partial x^4\partial t}+\frac{\partial^4 W_{(m)}}{\partial x^4}\frac{\partial^2 U_{(m)}}{\partial x\partial t}\right)+\\
&EAg(e_0a)^2\left(\frac{\partial^4 W_{(m)}}{\partial x^4}\frac{\partial^2 U_{(m)}}{\partial x\partial t}+3\frac{\partial^3 W_{(m)}}{\partial x^3}\frac{\partial^3 U_{(m)}}{\partial x^2\partial t}+3\frac{\partial^2 W_{(m)}}{\partial x^2}\frac{\partial^4 U_{(m)}}{\partial x^3\partial t}\right)-\\
&EAg\left(g\frac{\partial W_{(m)}}{\partial x}\frac{\partial^3 U_{(m)}}{\partial x^2\partial t}+g\frac{\partial^2 W_{(m)}}{\partial x^2}\frac{\partial^2 U_{(m)}}{\partial x\partial t}\right)-\left(EA+E^st^sA^s\right)\left(\frac{3}{2}\frac{\partial^2 W_{(m)}}{\partial x^2}\left(\frac{\partial W_{(m)}}{\partial x}\right)^2+\frac{\partial^2 W_{(m)}}{\partial x^2}\frac{\partial U_{(m)}}{\partial x}\right)-\\
&EAg\left(+2g\frac{\partial W_{(m)}}{\partial x}\frac{\partial^2 W_{(m)}}{\partial x^2}\frac{\partial^2 W_{(m)}}{\partial x\partial t}+g\left(\frac{\partial W_{(m)}}{\partial x}\right)^2\frac{\partial^3 W_{(m)}}{\partial x^2\partial t}\right)-\left(EA+E^st^sA^s\right)\left(\frac{\partial W_{(m)}}{\partial x}\frac{\partial^2 U_{(m)}}{\partial x^2}\right)-\\
&\tau^sA^s\left(\frac{\partial^2 W_{(m)}}{\partial x^2}-(e_0a)^2\frac{\partial^4 W}{\partial x^4}\right)+\tau^sA^s\left(\frac{1}{2}\left(\frac{\partial W}{\partial x}\right)^2+\frac{\partial^2 W}{\partial x^2}\left(\frac{\partial W}{\partial x}\right)^2\right)-\\
&\tau^sA^s(e_0a)^2\left(\frac{\partial W}{\partial x}\right)\left(\frac{\partial^4 W}{\partial x^4}\frac{\partial W}{\partial x}+3\frac{\partial^3 W}{\partial x^3}\frac{\partial^2 W}{\partial x^2}\right)-3\tau^sA^s(e_0a)^2\left(\frac{\partial^2 W}{\partial x^2}\right)\left(\frac{\partial^3 W}{\partial x^3}\frac{\partial W}{\partial x}+\left(\frac{\partial^2 W}{\partial x^2}\right)^2\right)-\\
&3\tau^sA^s(e_0a)^2\left(\frac{\partial^3 W}{\partial x^3}\right)\left(\frac{\partial W}{\partial x}\frac{\partial^2 W}{\partial x^2}\right)-\frac{\tau^sA^s(e_0a)^2}{2}\left(\frac{\partial^4 W}{\partial x^4}\right)\left(\frac{\partial W}{\partial x}\right)^2-(m_{(m)}+m_f)\frac{\partial^2 U_{(m)}}{\partial t^2}\frac{\partial W_{(m)}}{\partial x}+\\
&(e_0a)^2(m_{(m)}+m_f)\left\{\frac{\partial^4 U_{(m)}}{\partial x^2\partial t^2}\frac{\partial W_{(m)}}{\partial x}+\frac{\partial^3 U_{(m)}}{\partial x\partial t^2}\frac{\partial^2 W_{(m)}}{\partial x^2}+\frac{\partial^2 U_{(m)}}{\partial t^2}\frac{\partial^3 W_{(m)}}{\partial x^3}\right\}+m_fV_f\frac{\partial^2 W_{(m)}}{\partial x\partial t}\left(\frac{\partial W_{(m)}}{\partial x}\right)^2-\\
&(e_0a)^2m_fV_f\frac{\partial^4 W_{(m)}}{\partial x^3\partial t}\left(\frac{\partial W_{(m)}}{\partial x}\right)^2+2(e_0a)^2m_fV_f\frac{\partial^3 W_{(m)}}{\partial x^2\partial t}\frac{\partial^2 W_{(m)}}{\partial x^2}\frac{\partial W_{(m)}}{\partial x}+\\
&2(e_0a)^2m_fV_f\frac{\partial^3 W_{(m)}}{\partial x^3}\frac{\partial^2 W_{(m)}}{\partial x\partial t}\frac{\partial W_{(m)}}{\partial x}+m_fV_f^{\,2}\frac{\partial^2 W_{(m)}}{\partial x^2}\left(\frac{\partial W_{(m)}}{\partial x}\right)^2+(e_0a)^2m_fV_f\frac{\partial^2 W_{(m)}}{\partial x\partial t}\left(\frac{\partial W_{(m)}}{\partial x}\right)^2\left(\frac{\partial^2 W_{(m)}}{\partial x^2}\right)^2+\\
&(e_0a)^2m_fV_f\frac{\partial^2 W_{(m)}}{\partial x\partial t}\left(\frac{\partial^2 W_{(m)}}{\partial x^2}\right)^2-(e_0a)^2m_fV_f^{\,2}\frac{\partial^4 W_{(m)}}{\partial x^4}\left(\frac{\partial W_{(m)}}{\partial x}\right)^2+2(e_0a)^2m_fV_f^2\frac{\partial^3 W_{(m)}}{\partial x^3}\frac{\partial^2 W_{(m)}}{\partial x^2}\frac{\partial W_{(m)}}{\partial x}+\\
&(e_0a)^2m_fV_f^2\left(\frac{\partial^2 W_{(m)}}{\partial x^2}\right)^3\left(\frac{\partial W_{(m)}}{\partial x}\right)^2+EgI\;\frac{\partial^5 W_{(m)}}{\partial t\partial x^4}-\rho_tI\frac{\partial^4 W_{(m)}}{\partial x^2\partial t^2}+\rho_tI\;(e_0a)^2\frac{\partial^6 W_{(m)}}{\partial x^4\partial t^2}+(m_{(m)}+m_f)\frac{\partial^2 W_{(m)}}{\partial t^2}-
\end{aligned}
\tag{A.2}
$$

$$
\begin{aligned}
&(e_0a)^2(m_i+m_f)\frac{\partial^4 W_{(m)}}{\partial x^2\partial t^2}+2m_fV_f\frac{\partial^2 W_{(m)}}{\partial x\partial t}-2(e_0a)^2m_fU_f\frac{\partial^4 W_{(m)}}{\partial x^3\partial t}+(e_0a)^2m_fV_f\frac{\partial^4 W_{(m)}}{\partial x^4}\frac{\partial W_{(m)}}{\partial x}\frac{\partial W_{(m)}}{\partial t}-\\
&2m_fV_f\frac{\partial^2 W_{(m)}}{\partial x\partial t}-2(e_0a)^2m_fU_f\frac{\partial^4 W_{(m)}}{\partial x^3\partial t}+(e_0a)^2m_fV_f\frac{\partial^4 W_{(m)}}{\partial x^4}\frac{\partial W_{(m)}}{\partial x}\frac{\partial W_{(m)}}{\partial t}-(e_0a)^2m_fV_f\left(\frac{\partial^2 W_{(m)}}{\partial x^2}\right)^3\frac{\partial U_{(m)}}{\partial t}+\\
&(e_0a)^2m_fV_f\left(\frac{\partial^2 W_{(m)}}{\partial x^2}\right)^3\frac{\partial W_{(m)}}{\partial t}\frac{\partial W_{(m)}}{\partial x}+2(e_0a)^2m_fV_f\left(\frac{\partial^2 W_{(m)}}{\partial x^2}\right)^2\frac{\partial W_{(m)}}{\partial x\partial t}-m_fV_f\frac{\partial^2 W_{(m)}}{\partial x^2}\frac{\partial U_{(m)}}{\partial t}-\overline{\Pi}_0\frac{\partial^2 W_{(m)}}{\partial x^2}+\\
&(e_0a)\overline{\Pi}_0\frac{\partial^4 W_{(m)}}{\partial x^4}+h\frac{\partial^4 W_{(m)}}{\partial x^4}+3(e_0a)^2m_fV_f\frac{\partial^3 W_{(m)}}{\partial x^3}\frac{\partial^2 U_{(m)}}{\partial x\partial t}+3(e_0a)^2m_fV_f\frac{\partial^2 W_{(m)}}{\partial x^2}\frac{\partial^3 U_{(m)}}{\partial x^2\partial t}-\\
&3(e_0a)^2m_fV_f\frac{\partial^3 W_{(m)}}{\partial x^3}\frac{\partial^2 W_{(m)}}{\partial x^2}\frac{\partial W_{(m)}}{\partial x}\frac{\partial U_{(m)}}{\partial t}-3(e_0a)^2m_fV_f\left(\frac{\partial^2 W_{(m)}}{\partial x^2}\right)^2\frac{\partial W_{(m)}}{\partial x}\frac{\partial^2 U_{(m)}}{\partial x\partial t}+\\
&(e_0a)^2\rho_fI_f\frac{\partial^6 W_{(m)}}{\partial x^4\partial t^2}+m_fV_f^2\frac{\partial^2 W_{(m)}}{\partial x^2}-(e_0a)^2m_fV_f^2\frac{\partial^4 W_{(m)}}{\partial x^4}-k_wW_{(n)}+(e_0a)^2k_w\frac{\partial^2 W_{(n)}}{\partial x^2}+2k_wW_{(m)}\\
&2(e_0a)^2k_w\frac{\partial^2 W_{(m)}}{\partial x^2}+2C\frac{\partial W_{(m)}}{\partial t}-2(e_0a)^2C\frac{\partial^3 W_{(m)}}{\partial x^2\partial t}-C\frac{\partial W_{(n)}}{\partial t}+(e_0a)^2C\frac{\partial^3 W_{(n)}}{\partial x^2\partial t}-2G_P\frac{\partial^2 W_{(m)}}{\partial x^2}+\\
&2(e_0a)^2G_P\frac{\partial^4 W_{(m)}}{\partial x^4}+G_P\frac{\partial^2 W_{(n)}}{\partial x^2}-(e_0a)^2G_P\frac{\partial^4 W_{(n)}}{\partial x^4}-\eta_mH_x^{*2}\frac{\partial^2 W_{(m)}}{\partial x^2}+(e_0a)^2\eta_mH_x^{*2}\frac{\partial^4 W_{(m)}}{\partial x^4}+\\
&EgI\frac{\partial^5 W_{(m)}}{\partial x^4\partial t}+\mu A_f\frac{\partial^3 U_{(m)}}{\partial x^2\partial t}\frac{\partial W_{(m)}}{\partial x}+7(e_0a)^2\mu A_fV_f\frac{\partial^3 W_{(m)}}{\partial x^3}\left(\frac{\partial^2 W_{(m)}}{\partial x^2}\right)^2-\\
&4(e_0a)^2\mu A_fV_f\left(\frac{\partial^2 W_{(m)}}{\partial x^2}\right)^4\frac{\partial W_{(m)}}{\partial x}+7(e_0a)^2\mu A_fV_f\frac{\partial^4 W_{(m)}}{\partial x^4}\frac{\partial^2 W_{(m)}}{\partial x^2}\frac{\partial W_{(m)}}{\partial x}-\\
&(e_0a)^2\mu A_fV_f\left[\frac{\partial^5 U_{(m)}}{\partial x^4\partial t}\frac{\partial W_{(m)}}{\partial x}+\frac{\partial^4 U_{(m)}}{\partial x^3\partial t}\frac{\partial^2 W_{(m)}}{\partial x^2}+\frac{\partial^3 U_{(m)}}{\partial x^2\partial t}\frac{\partial^3 W_{(m)}}{\partial x^3}\right]+\\
&4(e_0a)^2\mu A_fV_f\frac{\partial^3 W_{(m)}}{\partial x^3}\left(\frac{\partial^2 W_{(m)}}{\partial x^2}\right)^2\left(\frac{\partial W_{(m)}}{\partial x}\right)^2+\mu V_fA_f\left\{-\frac{\partial^3 W_{(m)}}{\partial x^3}+\right.\\
&(e_0a)^2\mu U_fA_f\frac{\partial^5 W_{(m)}}{\partial x^5}-2(e_0a)^2\frac{\partial^4 W_{(m)}}{\partial x^4}\frac{\partial^2 W_{(m)}}{\partial x^2}\frac{\partial W_{(m)}}{\partial x}-(e_0a)^2\left(\frac{\partial^3 W_{(m)}}{\partial x^3}\right)^2\frac{\partial W_{(m)}}{\partial x}-\\
&(e_0a)^2\frac{\partial^3 W_{(m)}}{\partial x^3}\left(\frac{\partial^2 W_{(m)}}{\partial x^2}\right)^2+\left(\frac{\partial^2 W_{(m)}}{\partial x^2}\right)^2\frac{\partial W_{(m)}}{\partial x}-2(e_0a)^2\frac{\partial^4 W_{(m)}}{\partial x^4}\frac{\partial^2 W_{(m)}}{\partial x^2}\frac{\partial W_{(m)}}{\partial x}-\\
&\left.2(e_0a)^2\left(\frac{\partial^3 W_{(m)}}{\partial x^3}\right)^2\frac{\partial W_{(m)}}{\partial x}-5(e_0a)^2\frac{\partial^3 W_{(m)}}{\partial x^3}\left(\frac{\partial^2 W_{(m)}}{\partial x^2}\right)^2+(e_0a)^2\left(\frac{\partial^2 W_{(m)}}{\partial x^2}\right)^4\frac{\partial W_{(m)}}{\partial x}\right\}-\\
&\mu A_f\frac{\partial^3 W_{(m)}}{\partial x^2\partial t}+(e_0a)^2\mu A_f\frac{\partial^5 W_{(m)}}{\partial x^4\partial t}=0
\end{aligned}
\tag{A.2}
$$

After using dimensionless parameters the dimensional equations of motion can be converted to simple algebraic equation by applying DQ method. Eqs. (A. 3) and (A. 4) are algebraic equations of motion. $\delta u^{(m)}=0 \;\Rightarrow$

$$
\begin{aligned}
&-\sum_{k=1}^{N} C_{ik}^{2}u_k^{(m)}-\frac{1}{\eta}\sum_{k=1}^{N} C_{ik}^{2}w_k^{(m)}\sum_{k=1}^{N} C_{ik}w_k^{(m)}+\left(1+\rho f\right)\varpi^2\sum_{k=1}^{N} I_{ik}^{2}u_k^{(m)}-e_n^2\left(1+\rho f\right)\sum_{k=1}^{N} C_{ik}^{2}u_k^{(m)}-\\
&\frac{\sqrt{\rho}fV_f}{\eta}\varpi\sum_{k=1}^{N} C_{ik}u_k^{(m)}\sum_{k=1}^{N} C_{ik}u_k^{(m)}+\frac{e_n^2\sqrt{\rho}fV_f}{\eta}\varpi\sum_{k=1}^{N} C_{ik}^{3}w_k^{(m)}\sum_{k=1}^{N} C_{ik}w_k^{(m)}+\frac{e_n^2\sqrt{\rho}fV_f}{\eta}\varpi\sum_{k=1}^{N} C_{ik}w_k^{(m)}\sum_{k=1}^{N} C_{ik}^{3}w_k^{(m)}-\\
&\frac{2f\bar{\mu}V_f e_n^2}{\eta^2}\sum_{k=1}^{N} C_{ik}^{4}w_k^{(m)}\sum_{k=1}^{N} C_{ik}^{2}w_k^{(m)}-\frac{e_n^2\sqrt{\rho}fV_f}{\eta^3}\sum_{k=1}^{N} C_{ik}^{2}w_k^{(m)}\sum_{k=1}^{N} C_{ik}^{2}w_k^{(m)}\sum_{k=1}^{N} C_{ik}w_k^{(m)}+\\
&\frac{2e_n^2\sqrt{\rho}fV_f}{\eta}\varpi\sum_{k=1}^{N} C_{ik}^{2}w_k^{(m)}\sum_{k=1}^{N} C_{ik}^{2}w_k^{(m)}-\frac{fV_f^2}{\eta}\sum_{k=1}^{N} C_{ik}^{2}w_k^{(m)}\sum_{k=1}^{N} C_{ik}w_k^{(m)}+\frac{e_n^2fV_f^2}{\eta}\sum_{k=1}^{N} C_{ik}^{4}w_k^{(m)}\sum_{k=1}^{N} C_{ik}w_k^{(m)}+\\
&\frac{3e_n^2fV_f^2}{\eta}\varpi\sum_{k=1}^{N} C_{ik}^{2}w_k^{(m)}\sum_{k=1}^{N} C_{ik}^{3}w_k^{(m)}\sum_{k=1}^{N} C_{ik}w_k^{(m)}+\frac{f\bar{\mu}\sqrt{\rho}}{\eta^2}\sum_{k=1}^{N} C_{ik}^{3}w_k^{(m)}\sum_{k=1}^{N} C_{ik}w_k^{(m)}-\\
&\frac{e_n^2fV_f^2}{\eta^3}\sum_{k=1}^{N} C_{ik}^{2}w_k^{(m)}\sum_{k=1}^{N} C_{ik}^{2}w_k^{(m)}\sum_{k=1}^{N} C_{ik}^{2}w_k^{(m)}\sum_{k=1}^{N} C_{ik}w_k^{(m)}-\frac{\bar{\mu}\sqrt{\rho}f}{\eta}\varpi\sum_{k=1}^{N} C_{ik}^{2}w_k^{(m)}-\frac{\bar{\mu}\sqrt{\rho}fe_n^2}{\eta}\varpi\sum_{k=1}^{N} C_{ik}^{4}w_k^{(m)}+\\
&\frac{fV_f\bar{\mu}e_n^2}{\eta^2}\sum_{k=1}^{N} C_{ik}^{5}w_k^{(m)}\sum_{k=1}^{N} C_{ik}w_k^{(m)}+\frac{fV_f\bar{\mu}e_n^2}{\eta^2}\sum_{k=1}^{N} C_{ik}^{3}w_k^{(m)}\sum_{k=1}^{N} C_{ik}^{3}w_k^{(m)}-\frac{fV_f\bar{\mu}}{\eta^2}\sum_{k=1}^{N} C_{ik}^{2}w_k^{(m)}\sum_{k=1}^{N} C_{ik}^{2}w_k^{(m)}-\\
&\frac{g^*}{\eta}\varpi\sum_{k=1}^{N} C_{ik}^{2}w_k^{(m)}\sum_{k=1}^{N} C_{ik}w_k^{(m)}+\frac{2fV_f\bar{\mu}e_n^2}{\eta^2}\sum_{k=1}^{N} C_{ik}^{3}w_k^{(m)}\sum_{k=1}^{N} C_{ik}^{3}w_k^{(m)}-\\
&\frac{6fV_f\bar{\mu}e_n^2}{\eta^2}\sum_{k=1}^{N} C_{ik}^{3}w_k^{(m)}\sum_{k=1}^{N} C_{ik}^{2}w_k^{(m)}\sum_{k=1}^{N} C_{ik}^{2}w_k^{(m)}\sum_{k=1}^{N} C_{ik}w_k^{(m)}+\frac{2fV_f\bar{\mu}e_n^2}{\eta^2}\sum_{k=1}^{N} C_{ik}^{4}w_k^{(m)}\sum_{k=1}^{N} C_{ik}^{2}w_k^{(m)}+\\
&\frac{fV_f\bar{\mu}e_n^2}{\eta^4}\sum_{k=1}^{N} C_{ik}^{2}w_k^{(m)}\sum_{k=1}^{N} C_{ik}^{2}w_k^{(m)}\sum_{k=1}^{N} C_{ik}^{2}w_k^{(m)}\sum_{k=1}^{N} C_{ik}^{2}w_k^{(m)}-g^*\varpi\sum_{k=1}^{N} C_{ik}^{2}u_k^{(m)}-\frac{g^*}{\eta}\varpi\sum_{k=1}^{N} C_{ik}^{2}w_k^{(m)}\sum_{k=1}^{N} C_{ik}w_k^{(m)}=0,
\end{aligned}
\tag{A.3}
$$

and the transverse equations can be written as: $\delta w^{(m)}=0 \;\Rightarrow$

$$
\begin{aligned}
&-\left(1+\rho f\right)\frac{1}{\eta}\varpi^2\sum_{k=1}^{N} C_{ik}w_k^{(m)}\sum_{k=1}^{N} I_{ik}u_k^{(m)}+\left(1+\rho f\right)\frac{1}{\eta}e_n^2\varpi^2\left\{\sum_{k=1}^{N} C_{ik}w_k^{(m)}\sum_{k=1}^{N} C_{ik}^{2}u_k^{(m)}+\sum_{k=1}^{N} C_{ik}^{2}w_k^{(m)}\sum_{k=1}^{N} C_{ik}u_k^{(m)}\right\}+\\
&\left(1+\rho f\right)\frac{1}{\eta}e_n^2\varpi^2\left\{\sum_{k=1}^{N} C_{ik}^{3}w_k^{(m)}\sum_{k=1}^{N} I_{ik}u_k^{(m)}\right\}+V_ff\sqrt{\rho}\frac{1}{\eta^2}\varpi\left\{\sum_{k=1}^{N} C_{ik}w_k^{(m)}\sum_{k=1}^{N} C_{ik}w_k^{(m)}\sum_{k=1}^{N} C_{ik}w_k^{(m)}\right\}+\\
&e_n^2C_d\varpi\sum_{k=1}^{N} C_{ik}^{2}w_k^{(n)}-2e_n^2C_d\varpi\sum_{k=1}^{N} C_{ik}^{2}w_k^{(m)}+2e_n^2K_g\sum_{k=1}^{N} C_{ik}^{4}w_k^{(m)}+\\
&V_ff\sqrt{\rho}\frac{1}{\eta^2}\varpi\left\{-e_n^2\sum_{k=1}^{N} C_{ik}w_k^{(m)}\sum_{k=1}^{N} C_{ik}w_k^{(m)}\sum_{k=1}^{N} C_{ik}^{3}w_k^{(m)}+2e_n^2\sum_{k=1}^{N} C_{ik}w_k^{(m)}\sum_{k=1}^{N} C_{ik}^{2}w_k^{(m)}\sum_{k=1}^{N} C_{ik}^{2}w_k^{(m)}\right\}+\\
&V_ff\sqrt{\rho}\frac{1}{\eta^2}\varpi\left\{+2e_n^2\sum_{k=1}^{N} C_{ik}^{3}w_k^{(m)}\sum_{k=1}^{N} C_{ik}w_k^{(m)}\sum_{k=1}^{N} C_{ik}w_k^{(m)}+e_n^2\sum_{k=1}^{N} C_{ik}^{2}w_k^{(m)}\sum_{k=1}^{N} C_{ik}^{2}w_k^{(m)}\sum_{k=1}^{N} C_{ik}w_k^{(m)}\right\}+
\end{aligned}
\tag{A.4}
$$

$$
\begin{aligned}
&V_f f\sqrt{\rho}\,\frac{1}{\eta^4}\varpi e\sum_{k=1}^{N}C_{ik}^{2}w_k^{(m)}\sum_{k=1}^{N}C_{ik}^{2}w_k^{(m)}\sum_{k=1}^{N}C_{ik}w_k^{(m)}\sum_{k=1}^{N}C_{ik}w_k^{(m)}\sum_{k=1}^{N}C_{ik}w_k^{(m)}+\\
&fV_f^2\,\frac{1}{\eta^2}\sum_{k=1}^{N}C_{ik}^{2}w_k^{(m)}\sum_{k=1}^{N}C_{ik}w_k^{(m)}\sum_{k=1}^{N}C_{ik}w_k^{(m)}+\\
&fV_f^2\,\frac{1}{\eta^2}\left\{-e_n^2\sum_{k=1}^{N}C_{ik}^{4}w_k^{(m)}\sum_{k=1}^{N}C_{ik}w_k^{(m)}\sum_{k=1}^{N}C_{ik}w_k^{(m)}-2e_n^2\sum_{k=1}^{N}C_{ik}^{3}w_k^{(m)}\sum_{k=1}^{N}C_{ik}^{2}w_k^{(m)}\sum_{k=1}^{N}C_{ik}w_k^{(m)}\right\}+\\
&\frac{f\bar{\mu}V_f e_n^2}{\eta}\sum_{k=1}^{N}C_{ik}^{5}w_k^{(m)}+e_n^2 fV_f^2\,\frac{1}{\eta^4}\sum_{k=1}^{N}C_{ik}^{2}w_k^{(m)}\sum_{k=1}^{N}C_{ik}^{2}w_k^{(m)}\sum_{k=1}^{N}C_{ik}^{2}w_k^{(m)}\sum_{k=1}^{N}C_{ik}w_k^{(m)}\sum_{k=1}^{N}C_{ik}w_k^{(m)}-\\
&\frac{1}{\eta}\sum_{k=1}^{N}C_{ik}^{2}w_k^{(m)}\sum_{k=1}^{N}C_{ik}u_k^{(m)}+2C_d\varpi\sum_{k=1}^{N}I_{ik}w_k^{(m)}+\\
&\frac{1}{\eta}\left\{e_n^2\sum_{k=1}^{N}C_{ik}^{2}w_k^{(m)}\sum_{k=1}^{N}C_{ik}^{3}u_k^{(m)}+2e_n^2\sum_{k=1}^{N}C_{ik}^{3}w_k^{(m)}\sum_{k=1}^{N}C_{ik}^{2}u_k^{(m)}+e_n^2\sum_{k=1}^{N}C_{ik}^{4}w_k^{(m)}\sum_{k=1}^{N}C_{ik}u_k^{(m)}\right\}-\\
&\frac{f\bar{\mu}V_f}{\eta}\sum_{k=1}^{N}C_{ik}^{3}w_k^{(m)}--\frac{1}{2}\frac{1}{\eta^2}\sum_{k=1}^{N}C_{ik}^{2}w_k^{(m)}\sum_{k=1}^{N}C_{ik}w_k^{(m)}\sum_{k=1}^{N}C_{ik}w_k^{(m)}+\\
&3e_n^2\,\frac{1}{\eta^2}\sum_{k=1}^{N}C_{ik}^{2}w_k^{(m)}\sum_{k=1}^{N}C_{ik}^{3}w_k^{(m)}\sum_{k=1}^{N}C_{ik}w_k^{(m)}+\frac{\sqrt{\rho}f\mu e_n^2\varpi}{\eta}\sum_{k=1}^{N}C_{ik}^{4}w_k^{(m)}+\\
&e_n^2\,\frac{1}{\eta^2}\sum_{k=1}^{N}C_{ik}^{2}w_k^{(m)}\sum_{k=1}^{N}C_{ik}^{2}w_k^{(m)}\sum_{k=1}^{N}C_{ik}^{2}w_k^{(m)}+\frac{1}{2}\frac{e_n^2}{\eta^2}\sum_{k=1}^{N}C_{ik}^{4}w_k^{(m)}\sum_{k=1}^{N}C_{ik}w_k^{(m)}\sum_{k=1}^{N}C_{ik}w_k^{(m)}+\\
&\Delta\bar{T}\sum_{k=1}^{N}C_{ik}w_k^{(m)}-2K_g\sum_{k=1}^{N}C_{ik}^{2}w_k^{(m)}-e_n^2\Delta\bar{T}\sum_{k=1}^{N}C_{ik}^{4}w_k^{(m)}+\frac{\bar{I}}{\eta^2}\sum_{k=1}^{N}C_{ik}^{4}w_k^{(m)}-\frac{\bar{I}}{\eta^2}\varpi^2\sum_{k=1}^{N}C_{ik}^{2}w_k^{(m)}+\\
&e_n^2\,\frac{\bar{I}}{\eta^2}\varpi^2\sum_{k=1}^{N}C_{ik}^{4}w_k^{(m)}+\left(1+\rho f\right)\varpi^2\sum_{k=1}^{N}I_{ik}w_k^{(m)}-e_n^2\left(1+\rho f\right)\varpi^2\sum_{k=1}^{N}C_{ik}^{2}w_k^{(m)}+2\sqrt{\rho}fV_f\varpi\sum_{k=1}^{N}C_{ik}w_k^{(m)}-\\
&e_n^2\,2\sqrt{\rho}fV_f\varpi\sum_{k=1}^{N}C_{ik}^{3}w_k^{(m)}-\frac{\sqrt{\rho}f\bar{\mu}\varpi}{\eta}\sum_{k=1}^{N}C_{ik}^{2}w_k^{(m)}-C_d\varpi\sum_{k=1}^{N}I_{ik}w_k^{(n)}-\\
&\frac{\sqrt{\rho}\bar{\mu}fV_f}{\eta^2}\varpi\sum_{k=1}^{N}C_{ik}^{2}w_k^{(m)}\sum_{k=1}^{N}C_{ik}w_k^{(m)}\sum_{k=1}^{N}I_{ik}w_k^{(m)}+\frac{\sqrt{\rho}\bar{\mu}fV_f e_n^2}{\eta^2}\varpi\sum_{k=1}^{N}C_{ik}^{4}w_k^{(m)}\sum_{k=1}^{N}C_{ik}w_k^{(m)}\sum_{k=1}^{N}I_{ik}w_k^{(m)}-\\
&e_n^2K_g\sum_{k=1}^{N}C_{ik}^{4}w_k^{(n)}+\frac{3\sqrt{\rho}\bar{\mu}fV_f e_n^2}{\eta^2}\varpi\sum_{k=1}^{N}C_{ik}^{3}w_k^{(m)}\sum_{k=1}^{N}C_{ik}^{2}w_k^{(m)}\sum_{k=1}^{N}I_{ik}w_k^{(m)}+\\
&\frac{2\sqrt{\rho}\bar{\mu}fV_f e_n^2}{\eta^2}\varpi\sum_{k=1}^{N}C_{ik}^{2}w_k^{(m)}\sum_{k=1}^{N}C_{ik}^{2}w_k^{(m)}\sum_{k=1}^{N}C_{ik}w_k^{(m)}+K_g\sum_{k=1}^{N}C_{ik}^{2}w_k^{(n)}-\\
&\frac{\sqrt{\rho}\bar{\mu}fV_f e_n^2}{\eta^4}\varpi\sum_{k=1}^{N}C_{ik}^{2}w_k^{(m)}\sum_{k=1}^{N}C_{ik}^{2}w_k^{(m)}\sum_{k=1}^{N}C_{ik}^{2}w_k^{(m)}\sum_{k=1}^{N}C_{ik}w_k^{(m)}\sum_{k=1}^{N}I_{ik}w_k^{(m)}-\\
&\frac{\sqrt{\rho}fV_f}{\eta}\varpi\sum_{k=1}^{N}C_{ik}^{2}w_k^{(m)}\sum_{k=1}^{N}I_{ik}u_k^{(m)}+\frac{\sqrt{\rho}fV_f e_n^2}{\eta}\varpi\sum_{k=1}^{N}C_{ik}^{4}w_k^{(m)}\sum_{k=1}^{N}I_{ik}u_k^{(m)}+\\
&\frac{3\sqrt{\rho}fV_f e_n^2}{\eta}\varpi\sum_{k=1}^{N}C_{ik}^{3}w_k^{(m)}\sum_{k=1}^{N}C_{ik}u_k^{(m)}+\frac{3\sqrt{\rho}fV_f e_n^2}{\eta}\varpi\sum_{k=1}^{N}C_{ik}^{3}w_k^{(m)}\sum_{k=1}^{N}C_{ik}^{2}u_k^{(m)}-\\
&\frac{3\sqrt{\rho}fV_f e_n^2}{\eta^3}\varpi\sum_{k=1}^{N}C_{ik}w_k^{(m)}\sum_{k=1}^{N}C_{ik}^{2}w_k^{(m)}\sum_{k=1}^{N}C_{ik}^{3}w_k^{(m)}\sum_{k=1}^{N}I_{ik}u_k^{(m)}-\\
&\frac{3\sqrt{\rho}fV_f e_n^2}{\eta^3}\varpi\sum_{k=1}^{N}C_{ik}^{2}w_k^{(m)}\sum_{k=1}^{N}C_{ik}^{2}w_k^{(m)}\sum_{k=1}^{N}C_{ik}w_k^{(m)}\sum_{k=1}^{N}C_{ik}u_k^{(m)}-
\end{aligned}
\qquad (A.4)
$$

$$
\begin{aligned}
&\frac{\sqrt{\rho} f V_f e_n^2}{\eta^3}\varpi \sum_{k=1}^{N} C_{ik}^2 w_k^{(m)} \sum_{k=1}^{N} C_{ik}^2 u_k^{(m)} \sum_{k=1}^{N} C_{ik}^2 w_k^{(m)} \sum_{k=1}^{N} I_{ik} u_k^{(m)} - \\
&\frac{\sqrt{\rho} f V_f}{\eta}\varpi \sum_{k=1}^{N} C_{ik} w_k^{(m)} \sum_{k=1}^{N} C_{ik} u_k^{(m)} - \frac{\rho f \bar{I}_f}{\eta^2}\varpi^2 \sum_{k=1}^{N} C_{ik}^2 w_k^{(m)} + \\
&\frac{e_n^2\sqrt{\rho} f V_f}{\eta}\varpi \sum_{k=1}^{N} C_{ik} w_k^{(m)} \sum_{k=1}^{N} C_{ik}^3 u_k^{(m)} + \frac{e_n^2 \rho f \bar{I}_f}{\eta^2}\varpi^2 \sum_{k=1}^{N} C_{ik}^4 w_k^{(m)} + \frac{\bar{\mu}\sqrt{\rho} f}{\eta^2}\varpi \sum_{k=1}^{N} C_{ik} w_k^{(m)} \sum_{k=1}^{N} C_{ik}^2 u_k^{(m)} + \\
&\frac{7e_n^2 V_f f\bar{\mu}}{\eta^3} \sum_{k=1}^{N} C_{ik}^4 w_k^{(m)} \sum_{k=1}^{N} C_{ik}^2 w_k^{(m)} \sum_{k=1}^{N} C_{ik} w_k^{(m)} + \frac{7e_n^2 V_f f\bar{\mu}}{\eta^3} \sum_{k=1}^{N} C_{ik}^3 w_k^{(m)} \sum_{k=1}^{N} C_{ik}^2 w_k^{(m)} \sum_{k=1}^{N} C_{ik}^2 w_k^{(m)} - \\
&\frac{4e_n^2 V_f f\bar{\mu}}{\eta^5} \sum_{k=1}^{N} C_{ik}^2 w_k^{(m)} \sum_{k=1}^{N} C_{ik}^2 w_k^{(m)} \sum_{k=1}^{N} C_{ik}^2 w_k^{(m)} \sum_{k=1}^{N} C_{ik}^2 w_k^{(m)} \sum_{k=1}^{N} C_{ik} w_k^{(m)} + \\
&\frac{4e_n^2 V_f f\bar{\mu}}{\eta^3} \sum_{k=1}^{N} C_{ik}^5 w_k^{(m)} \sum_{k=1}^{N} C_{ik} w_k^{(m)} \sum_{k=1}^{N} C_{ik} w_k^{(m)} + \frac{3e_n^2 V_f f\bar{\mu}}{\eta^3} \sum_{k=1}^{N} C_{ik}^3 w_k^{(m)} \sum_{k=1}^{N} C_{ik}^3 w_k^{(m)} \sum_{k=1}^{N} C_{ik} w_k^{(m)} - \\
&\frac{4e_n^2 V_f f\bar{\mu}}{\eta^5} \sum_{k=1}^{N} C_{ik}^3 w_k^{(m)} \sum_{k=1}^{N} C_{ik}^2 w_k^{(m)} \sum_{k=1}^{N} C_{ik}^2 w_k^{(m)} \sum_{k=1}^{N} C_{ik} w_k^{(m)} \sum_{k=1}^{N} C_{ik} w_k^{(m)} - \\
&\frac{V_f f\bar{\mu}}{\eta^3} \sum_{k=1}^{N} C_{ik}^3 w_k^{(m)} \sum_{k=1}^{N} C_{ik} w_k^{(m)} \sum_{k=1}^{N} C_{ik} w_k^{(m)} - \frac{V_f f\bar{\mu}}{\eta^3} \sum_{k=1}^{N} C_{ik}^2 w_k^{(m)} \sum_{k=1}^{N} C_{ik}^2 w_k^{(m)} \sum_{k=1}^{N} C_{ik} w_k^{(m)} - \\
&\frac{e_n^2\bar{\mu} f\sqrt{\rho}}{\eta^2}\varpi \sum_{k=1}^{N} C_{ik}^2 w_k^{(m)} \sum_{k=1}^{N} C_{ik}^3 u_k^{(m)} - \frac{e_n^2\bar{\mu} f\sqrt{\rho}}{\eta^2}\varpi \sum_{k=1}^{N} C_{ik}^3 w_k^{(m)} \sum_{k=1}^{N} C_{ik}^2 u_k^{(m)} - \\
&\frac{4e_n^2 f V_f\bar{\mu}}{\eta^3} \sum_{k=1}^{N} C_{ik}^4 w_k^{(m)} \sum_{k=1}^{N} C_{ik}^2 w_k^{(m)} \sum_{k=1}^{N} C_{ik} w_k^{(m)} - \frac{3e_n^2 f V_f\bar{\mu}}{\eta^3} \sum_{k=1}^{N} C_{ik}^3 w_k^{(m)} \sum_{k=1}^{N} C_{ik}^3 w_k^{(m)} \sum_{k=1}^{N} C_{ik} w_k^{(m)} + \\
&\frac{f V_f\bar{\mu}}{\eta^3} \sum_{k=1}^{N} C_{ik}^2 w_k^{(m)} \sum_{k=1}^{N} C_{ik}^2 w_k^{(m)} \sum_{k=1}^{N} C_{ik} w_k^{(m)} + 2k_w \sum_{k=1}^{N} I_{ik} w_k^{(m)} - k_w \sum_{k=1}^{N} I_{ik} w_k^{(n)} + e_n^2 k_w \sum_{k=1}^{N} C_{ik}^2 w_k^{(n)} - \\
&2e_n^2 k_w \sum_{k=1}^{N} C_{ik}^2 w_k^{(m)} - \frac{e_n^2\bar{\mu} f\sqrt{\rho}}{\eta^2}\varpi \sum_{k=1}^{N} C_{ik} w_k^{(m)} \sum_{k=1}^{N} C_{ik}^4 u_k^{(m)} - \frac{6e_n^2 f V_f\bar{\mu}}{\eta^3} \sum_{k=1}^{N} C_{ik}^2 w_k^{(m)} \sum_{k=1}^{N} C_{ik}^2 w_k^{(m)} \sum_{k=1}^{N} C_{ik}^3 w_k^{(m)} + \\
&\frac{e_n^2 f V_f\bar{\mu}}{\eta^5} \sum_{k=1}^{N} C_{ik}^2 w_k^{(m)} \sum_{k=1}^{N} C_{ik}^2 w_k^{(m)} \sum_{k=1}^{N} C_{ik}^2 w_k^{(m)} \sum_{k=1}^{N} C_{ik}^2 w_k^{(m)} \sum_{k=1}^{N} C_{ik} w_k^{(m)} + \frac{\bar{h}}{\eta^2} \sum_{k=1}^{N} C_{ik}^4 w_k^{(m)} - \bar{\Pi}_0 \sum_{k=1}^{N} C_{ik}^2 w_k^{(m)} + \\
&e_n^2\bar{\Pi}_0 \sum_{k=1}^{N} C_{ik}^4 w_k^{(m)} - H_x^* \sum_{k=1}^{N} C_{ik}^2 w_k^{(m)} + H_x^* e_n^2 \sum_{k=1}^{N} C_{ik}^4 w_k^{(m)} + f V_f^2 \sum_{k=1}^{N} C_{ik}^2 w_k^{(m)} - e_n^2 f V_f^2 \sum_{k=1}^{N} C_{ik}^4 w_k^{(m)} + \\
&\frac{e_n^2\bar{I}}{\eta^2}\varpi^2 \sum_{k=1}^{N} C_{ik}^4 w_k^{(m)} - \frac{\bar{I}}{\eta^2}\varpi^2 \sum_{k=1}^{N} C_{ik}^2 w_k^{(m)} + \frac{\rho e_n^2 f\bar{I}_f}{\eta^2}\varpi^2 \sum_{k=1}^{N} C_{ik}^4 w_k^{(m)} - \frac{\rho f\bar{I}_f}{\eta^2}\varpi^2 \sum_{k=1}^{N} C_{ik}^2 w_k^{(m)} + \\
&\frac{\bar{I} g^*}{\eta^2}\varpi \sum_{k=1}^{N} C_{ik}^4 w_k^{(m)} - e_n^2\Delta\bar{T} g^*\varpi \sum_{k=1}^{N} C_{ik}^4 w_k^{(m)} + \Delta\bar{T} g^*\varpi \sum_{k=1}^{N} C_{ik}^2 w_k^{(m)} - \frac{g^*}{\eta}\varpi \sum_{k=1}^{N} C_{ik}^2 w_k^{(m)} \sum_{k=1}^{N} C_{ik} u_k^{(m)} - \\
&\frac{g*}{\eta}\varpi \sum_{k=1}^{N} C_{ik}^2 w_k^{(m)} \sum_{k=1}^{N} C_{ik} u_k^{(m)} + \frac{e_n^2 g^*}{\eta}\varpi \sum_{k=1}^{N} C_{ik}^2 w_k^{(m)} \sum_{k=1}^{N} C_{ik}^3 u_k^{(m)} + \frac{2e_n^2 g^*}{\eta}\varpi \sum_{k=1}^{N} C_{ik}^3 w_k^{(m)} \sum_{k=1}^{N} C_{ik}^2 u_k^{(m)} + \\
&\frac{e_n^2 g^*}{\eta}\varpi \sum_{k=1}^{N} C_{ik}^4 w_k^{(m)} \sum_{k=1}^{N} C_{ik} u_k^{(m)} + \frac{e_n^2 g^*}{\eta}\varpi \sum_{k=1}^{N} C_{ik}^4 w_k^{(m)} \sum_{k=1}^{N} C_{ik} u_k^{(m)} - \\
&\frac{g^*}{2\eta^2}\varpi \sum_{k=1}^{N} C_{ik} w_k^{(m)} \sum_{k=1}^{N} C_{ik} w_k^{(m)} \sum_{k=1}^{N} C_{ik}^2 w_k^{(m)} - \frac{g^*}{\eta^2}\varpi \sum_{k=1}^{N} C_{ik}^2 w_k^{(m)} \sum_{k=1}^{N} C_{ik} w_k^{(m)} \sum_{k=1}^{N} C_{ik} w_k^{(m)} +
\end{aligned}
\tag{A.4}
$$

$$\frac{3e_n^2g^*}{\eta^2}\varpi\sum_{k=1}^{N}C_{ik}^2w_k^{(m)}\sum_{k=1}^{N}C_{ik}w_k^{(m)}\sum_{k=1}^{N}C_{ik}^3w_k^{(m)}+\frac{3e_n^2g^*}{\eta^2}\varpi\sum_{k=1}^{N}C_{ik}^3w_k^{(m)}\sum_{k=1}^{N}C_{ik}^2w_k^{(m)}\sum_{k=1}^{N}C_{ik}w_k^{(m)}+$$
$$\frac{3e_n^2g^*}{\eta^2}\varpi\sum_{k=1}^{N}C_{ik}^3w_k^{(m)}\sum_{k=1}^{N}C_{ik}^2w_k^{(m)}\sum_{k=1}^{N}C_{ik}w_k^{(m)}+\frac{3e_n^2g^*}{\eta^2}\varpi\sum_{k=1}^{N}C_{ik}^2w_k^{(m)}\sum_{k=1}^{N}C_{ik}^2w_k^{(m)}\sum_{k=1}^{N}C_{ik}^2w_k^{(m)}+ \quad (A.4)$$
$$\frac{e_n^2g^*}{2\eta^2}\varpi\sum_{k=1}^{N}C_{ik}w_k^{(m)}\sum_{k=1}^{N}C_{ik}w_k^{(m)}\sum_{k=1}^{N}C_{ik}^4w_k^{(m)}+\frac{e_n^2g^*}{\eta^2}\varpi\sum_{k=1}^{N}C_{ik}w_k^{(m)}\sum_{k=1}^{N}C_{ik}^4w_k^{(m)}\sum_{k=1}^{N}C_{ik}w_k^{(m)}=0.$$

REFERENCES

[1] Iijima S., 1991, Helical microtubules of graphitic carbon, *Nature* **354**: 56-58.
[2] Lim C.W., Li C., Yu J.L., 2010, Dynamic behavior of axially moving nanobeams based on nonlocal elasticity approach, *Acta Mechanica Sinica* **26**: 755-265.
[3] Zhen Y., Fang B., 2010, Thermal–mechanical and nonlocal elastic vibration of single-walled carbon nanotubes conveying fluid, *Computational Materials Science* **49**: 276-282.
[4] Fang B., Xin Y., Zhen C., Ping Z., Tang Y., 2013, Nonlinear vibration analysis of double-walled carbon nanotubes based on nonlocal elasticity theory, *Applied Mathematical Modelling* **37**: 1096-1107.
[5] Wang L., Ni Q., 2009, A reappraisal of the computational modelling of carbon nanotubes conveying viscous fluid, *Mechanics Research Communications* **36**:833-837.
[6] Soltani P., Farshidianfar A., 2012, Periodic solution for nonlinear vibration of a fluid-conveying carbon nanotube, based on the nonlocal continuum theory by energy balance method, *Applied Mathematical Modelling* **36**: 3712-3724.
[7] Ghorbanpour Arani A., Shajari A.R., Amir S., Loghman A., 2012, Electro-thermo-mechanical nonlinear nonlocal vibration and instability of embedded micro-tube reinforced by BNNT, conveying fluid, *Physica E* **45**: 109-121.
[8] Mirramezani M., Mirdamadi H.R., 2012, The effects of Knudsen-dependent flow velocity on vibrations of a nano-pipe conveying fluid, *Archive of Applied Mechanics* **82**: 879-890.
[9] Rashidi V., Mirdamadi H.R., Shirani E., 2012, A novel model for vibrations of nanotubes conveying nano flow, *Computational Materials Science* **51**: 347-352.
[10] Wang L., 2010, Vibration analysis of fluid-conveying nanotubes with consideration of surface effect, *Physica E* **43**: 437-439.
[11] Gurtin M.E., Murdoch A.I., 1975, A continuum theory of elastic material surface, *Archive for Rational Mechanics and Analysis* **57**(4): 291-323.
[12] Gurtin M.E., Murdoch A.I., 1978, Surface stress in solids, *International Journal of Solids and Structures* **14**(6): 431-440.
[13] Lei Y., Adhikari S., Friswell M.I., 2013, Vibration of nonlocal Kelvin–Voigt viscoelastic damped Timoshenko beams, *International Journal of Engineering Science* **66/67**: 1-13.
[14] Ghavanloo E., Fazelzadeh S.A., 2011, Flow-thermo elastic vibration and instability analysis of viscoelastic carbon nanotubes embedded in viscous fluid, *Physica E* **44**: 17-24.
[15] Murmu T., McCarthy M.A., Adhikari S., 2012, Vibration response of double-walled carbon nanotubes subjected to an externally applied longitudinal magnetic field: A nonlocal elasticity approach, *Journal of Sound and Vibration* **331**: 5069-5086.
[16] Wang H., Dong K., Men F., Yan Y.J., Wang X., 2010, Influences of longitudinal magnetic field on wave propagation in carbon nanotubes embedded in elastic matrix, *Applied Mathematical Modelling* **34**: 878-889.
[17] Murmu T., McCarthy M.A., Adhikari S., 2013, In-plane magnetic field affected transverse vibration of embedded single-layer graphene sheets using equivalent nonlocal elasticity approach, *Composite Structures* **96**: 57-63.
[18] Murmu T., Adhikari S., 2011, Axial instability of double-nanobeam-systems, *Physics Letters A* **375**: 601-608.
[19] Murmu T., Adhikari S., 2010, Nonlocal transverse vibration of double-nanobeam-systems, *Journal of Applied Physics* **108**: 083514.
[20] Murmu T., Adhikari S., 2010, Nonlocal effects in the longitudinal vibration of double-nanorod systems, *Physica E* **43**: 415-422.
[21] Murmu T., Adhikari S., 2011, Nonlocal vibration of bonded double-nanoplate-systems, *Composites Part B: Engineering* **42**:1901-1911.
[22] Ghorbanpour Arani A., Amir S., 2013, Electro-thermal vibration of visco-elastically coupled BNNT systems conveying fluid embedded on elastic foundation via strain gradiant theory, *Physica B* **419**: 1-6.
[23] Eringen A.C., Edelen D.G.B., 1972, On nonlocal elasticity, *International Journal of Engineering Science* **10**: 233-248.
[24] Eringen A.C., 1983, On differential equations of nonlocal elasticity and solutions of screw dislocation and surface wave, *Journal of Applied Physics* **54**: 4703-4710.
[25] Reddy J.N., 2002, *Energy Principles and Variational Methods in Applied Mechanics*, John Willey & Sons.

[26] Reddy J.N., Wang C.M., 2004, dynamics of fluid conveying beams, *Centre for Offshore Research and Engineering National University of Singapore*.

[27] Khodami Maraghi Z., Ghorbanpour Arani A., Kolahchi R., Amir S., Bagheri M.R., 2013, Nonlocal vibration and instability of embedded DWBNNT conveying viscose fluid, *Composites Part B: Engineering* **45**: 423-432.

[28] Wang L., Ni Q., 2009, A reappraisal of the computational modelling of carbon nanotubes conveying viscous fluid, *Mechanics Research Communications* **36**: 833-837.

[29] Paidoussis M.D., 1998, *Fluid-Structure Interactions: Slender Structures and Axial Flow*, Academic Press, London.

[30] Beskok A., Karniadakis G.E., 1999, Report: a model for flows in channels, pipes, and ducts at micro and nano scales, *Microscale Thermophysical Engineering* **3**: 43-77.

[31] Ghorbanpour Arani A., Loghman A., Shajari A.R., Amir S., 2010, Semi-analytical solution of magneto-thermo-elastic stresses for functionally graded variable thickness rotating disks, *Journal of Mechanical Science and Technology* **24**: 2107-2117.

[32] Bellman R.E., Kashef B.G., Casti J., 1972, Differential quadrature: A technique for the rapid solution of nonlinear partial differential equations, *Journal of Computational Physics* **10**: 40-52.

[33] Hu L.C., Hu C., 2013, Identification of rate constants by differential quadrature in partly measurable compartmental models, *Mathematical Biosciences* **21**: 71-76.

[34] Civan F., Sliepcevich C.M., 1984, Application of differential quadrature to transport processes, *Journal of Mathematical Analysis and Applications* **101**: 423-443.

[35] Striz A.G., Jang S.K., Bert C.W., 1988, Nonlinear bending analysis of thin circular plates by differential quadrature, *Thin-walled structures* **6**: 51-62.

[36] Bozdogan K.B., 2012, Differential quadrature method for free vibration analysis of coupled shear walls, *Structural Engineering & Mechanics* **41**: 67-81.

[37] Girgin Z., Yilmaz Y., Cetkin A., 2000, Application of the generalized differential quadrature method to deflection and buckling analysis of structural components, *International Journal of Engineering Science* **6**: 117-124.

[38] Chen W., Zhong T., 1997, The study on nonlinear computations of the DQ and DC methods, *Numerical Methods for Partial Differential Equations* **13**: 57-75.

[39] Johnson C.R., 1989, *Matrix Theory and Application*, Phoenix, Arizona.

[40] Shu C., 1999, *Differential Quadrature and its Application in Engineering*, Springer.

[41] Ghorbanpour Arani A., Atabakhshian V., Loghman A., Shajari A.R., Amir S., 2012, Nonlinear vibration of embedded SWBNNTs based on nonlocal Timoshenko beam theory using DQ method, *Physica B* **407**: 2549-2555.

[42] Sharma P., Parashar S.K., Rathore S.K., 2012, Application of DQ method in certain class of vibration problem, *International Conference on Mechanical and Industrial Engineering*, Dehradun.

[43] Yoon J., Ru C.Q., Mioduchowski A., 2005, Vibration and instability of carbon nanotubes conveying fluid, *Composites Science and Technology* **65**: 1326-1336.

[44] Wang L., Ni Q., Li M., Qian Q., 2008, The thermal effect on vibration and instability of carbon nanotubes conveying fluid, *Physica E* **40**: 3179-3182.